BIOPHYSICAL STUDIES OF THE INTERACTIONS OF SEVERAL BIOACTIVE LIPIDS IN MODEL MEMBRANES

by

Evan A. Mintzer

A dissertation submitted to the Graduate Faculty in Biochemistry in partial fulfillment of the requirements for the degree of Doctor of Philosophy, The City University of New York.

2006

This manuscript has been read and accepted for the

Graduate Faculty in Biochemistry in satisfaction of the

dissertation requirement for the degree of Doctor of Philosophy.

Evan A. Mintzer

10-21-05
Date

Dr. Robert Bittman
Chair of Examining Committee

10-21-05
Date

Dr. Leslie Davenport
Executive Officer

Dr. Fred Naider

Dr. Ruth Stark

Dr. Michael Palmer

Dr. Probal Banerjee
Supervision Committee

THE CITY UNIVERSITY OF NEW YORK

The City University of New York

Abstract

BIOPHYSICAL STUDIES OF THE INTERACTIONS OF SEVERAL BIOACTIVE LIPIDS IN MODEL MEMBRANES

By

Evan A. Mintzer

Advisor: Professor Robert Bittman

The use of model systems affords the researcher an opportunity to study the complex topic of membrane dynamics and structure under controlled conditions. The investigation into an array of the properties of a small group of bioactive lipids was undertaken, and is summarized in Chapter 1. Isothermal titration calorimetry, compression of lipid monolayers, detergent solubility, and cyclodextrin-mediated efflux assays were used to investigate some of the properties of cholesterol analogs and oxidized sterols, lysophosphatidic acid (LPA), and lipopolysaccharide (LPS).

In Chapter 2, the properties of a photoactivatable derivative and fluorescent analogs of cholesterol were examined to assess their ability to faithfully mimic the parent molecule in model membrane systems. The photoactivatable probe, 6-photocholesterol, behaved in a manner similar to cholesterol. Two structurally

related novel fluorescent cholesterol analogs were also examined: one, in which a BODIPY fluorophore is attached via an ester linkage, differed from cholesterol with respect to lipid-lipid interactions and may localize into non-raft domains in fluorescence studies; the other, coupled to the fluorophore without polar atoms, possessed properties that resembled those of cholesterol and appears to have utility as a membrane mimetic probe. The enantiomer of cholesterol interacted with phospholipids in monolayers and vesicles in a similar manner as cholesterol, as discussed in Chapter 3.

Results reported in Chapter 4 reveal significant variations between cholesterol and several of its oxidized products with regard to condensation of 1-palmitoyl-2-oleoyl-*sn*-glycero-3-phosphocholine monolayers and support of the formation of detergent-resistant lipid rafts.

Chapter 5 presents an isothermal titration calorimetric study of the equilibrium binding of LPA, a structurally simple lipid molecule with wide ranging biological activities, to the lipid-binding domain of the actin-severing protein gelsolin, denoted as P2. A strong dependence for LPA-gelsolin interactions on salt concentration and LPA structure was found, suggesting a high degree of specificity of the peptide for this lipid. P2 has a higher affinity for LPS from *P. aeruginosa* than for 1-oleoyl-LPA.

Calorimetric measurements of the critical micelle concentrations (CMC) of LPA and sphingosylphosphorylcholine (SPC) are presented in Chapter 6. A dependence on salt concentration and structure was revealed for LPA, but no such salt sensitivity was observed for SPC. However, reduction of the double bond in SPC lowered the CMC by a factor of three.

Acknowledgments

I would like to thank the following scientists for their generous supply of reagents and expertise: Professor Fred Naider and Dr. Hasmik Sargsyan (P2 peptide), College of Staten Island - CUNY, Staten Island, NY; Professor Paul A. Janmey (gelsolin, P2 peptide), University of Pennsylvania School of Medicine, Philadelphia, PA; Professor Jan Wilschut and Dr. Barry-Lee Waarts (viral fusion assay), University of Groningen, Groningen, The Netherlands; Dr. Zaiguo Li (BODIPY-cholesterol analogs and ITC), Queens College, CUNY, Flushing, NY; Professor Erwin London and Ms. Mehga (fluorescence assay), State University of New York at Stony Brook, Stony Brook, NY; Professor Howard L. Brockman (monolayer expertise), Hormel Institute, Austin, MN; Professor Douglas Covey (enantiomeric cholesterol), Washington University School of Medicine, St. Louis, MO.

I dedicate this dissertation to:

- Distinguished Professor Robert Bittman, for his unending patience and guidance. The true definition of the word "Mentor,"
- My committee members, Professors Fred Naider, Ruth Stark, Probal Banerjee, and Michael Palmer, for their support through these long years,
- The faculty at Queens College - CUNY, especially Professors Wilma Saffran, Thomas Strekas, William Hersh, Robert Engel, David Baker, and Harry Gafney for providing the spark to take the first steps on this long, strange trip,
- The faculty at Clayton State University for recognizing talent,
- My mother, father, and sister Jennifer, for their support (financial and otherwise), who are all *kvelling*, in this world and the next one,
- My beautiful boys Matthew, Ryan, Justin, and Elijah Mintzer for their understanding during these years of Dad not being home enough,

and, most especially,

♥ My wonderful wife and life's partner Dianela, for standing by my side while I followed a dream, for her Job-like patience through lonely nights and kid-filled days, for stretching dollars to pay bills in ways I still don't understand, for persevering through the most troubled times, and for giving me the love that no human deserves:

"…a love like ours could never die

as long as I have her near me

and I love her".

Lennon and McCartney

Table of Contents

List of Figures and Tables

Chapter 2

Part 1

Part 2

Chapter 3

Chapter 4

Chapter 5

Chapter 6

List of Abbreviations

BODIPY, borondipyrromethane (4,4-difluoro-4-bora-3a,4a-diaza-*s*-indacenes)

CMC, critical micelle concentration

CPD-1, BODIPY-cholesterol analog 1

CPD-2, BODIPY-cholesterol analog 2

DRM, detergent-resistant membranes

EDG, Endothelial Differentiation Genes

ent-cholesterol, enantiomeric cholesterol

ESPM, egg sphingomyelin

GPCR, G-protein coupled receptors

HPCD, 2-hydroxypropyl-β-cyclodextrin

ITC, isothermal titration calorimetry

LBP, LPS-binding protein

LPA, 1-acyl-2-hydroxy-s*n*-glycero-3-phosphate

LPC, 1-acyl-2-hydroxy-s*n*-glycero-3-phosphocholine

LPS, lipopolysaccharide

LUV, large unilamellar vesicles

MLV, multilamellar vesicles

MSPM, milk sphingomyelin

OD, optical density

PIP_2, phosphatidylinositol-4,5-bisphosphate

POPC, 1-palmitoyl-2-oleoyl-s*n*-glycero-3-phosphocholine

SFV, Semliki Forest virus

SIN, Sindbis virus

SPC, sphingosylphosphorylcholine

Chapter 1

Introduction: Biophysical Studies of the Interactions of Several Bioactive Lipids in Model Membranes

"Lipidomics," a phrase that only several years ago may not have been recognizable, is now one of the most active areas of biochemical and biophysical research (*1*), as judged by the number of hits in a Google search (>8,000) as of the writing of this thesis (September 2005). Far from occupying the position of mere membrane structural scaffolding, lipids have been implicated in a vast number of pathologies, including cancer (*2*), diabetes (*3*), sepsis (*4*), neurodegenerative disorders (*5*), and heart disease (*6*). Lipid second messengers (*7*) and membrane receptors (*8*) that are associated with lipids are well known. The structural diversity of lipids, from simple (e.g., lysophosphatidic acid, MW ~458) to complex (e.g., lipopolysaccharides, (MW ~5 kDa-25 kDa), hints at the myriad of possible ways in which they can interact with other cellular components and chemical species.

This thesis describes the findings of biophysical studies in model membranes designed to obtain a more complete understanding of how a small sample group of lipids interacts with other lipids and with the lipid-binding domain of the cellular protein gelsolin. The results of studies with lipid molecules bearing reporter moieties are also presented. The focus of the projects described herein is to add to our understanding of the behavior and properties of several bioactive lipids. I have endeavored to examine an extremely complex topic using biophysical methods (principally isothermal titration calorimetry and monolayer compression).

The use of model membranes allows the researcher to control conditions to a degree not possible using in vivo assays (*9*). A vast amount of extremely significant data have been collected using this approach, the import of which cannot be overstated (see, e.g., (*9-13*)). It is the hope of the author that this brief glimpse into the complicated world of biomembranes, using the tools at his disposal and several representative compounds, will be useful in future research on these bioactive lipids.

Membrane research using reporter lipid molecules is a powerful technique for elucidating the function and structure of biological species and processes (see, e.g., (*14*)). These methods, however, are limited in their utility by their potential to cause perturbations in the natural environment as a result of added fluorophores or other chemical modifications. Thus, their use relies on the ability of the reporter molecules to behave as closely as possible to the parent molecule they were designed to mimic. Chapter 2 of this thesis discusses the results of a study of the behavior of cholesterol analogs using Langmuir monolayers, a detergent solubility assay and a cyclodextrin-mediated sterol adsorption assay. Part 1 of Chapter 2 describes a published project (*15*) involving the behavior of a photoactivatable analog bearing a diazirine functionality (a carbene precursor) at the C6 of cholestanol (termed 6-photocholesterol). The results suggest that the probe mimics the behavior of cholesterol in monomolecular films with respect to its ability to condense diacylphosphatidylcholine monolayers at the air-water interface. Additional support for this conclusion was provided by collaborators from the University Medical Center at Groningen, The Netherlands, who used a low pH induced membrane fusion assay

to show that 6-photocholesterol mediated the fusion of two viral membranes to large unilamellar vesicles to an extent similar to native cholesterol.

Part 2 of Chapter 2 describes several biophysical properties of two fluorescent cholesterol analogs bearing a BODIPY moiety in the aliphatic side chain. The compounds differ from each other in the way they are linked to the side chain, with one attached via an ester linkage and the other devoid of any oxygen atoms. Using pure and mixed monolayers, a detergent-solubility assay, and a cyclodextrin efflux assay, we found that the oxygen atoms in the side chain interfered with sterol-lipid interactions. The analog linked without the ester mixed ideally with phospholipids (but did not induce condensation in monolayers), supported insoluble domain formation in multilamellar vesicles to an extent similar to cholesterol, and displayed comparable kinetics to cholesterol in the cyclodextrin-mediated efflux from POPC-sterol binary monolayers. It was concluded that the ester-linked analog may have utility as a negative control for cholesterol, and the non-ester compound, by virtue of its cholesterol-like properties, may be used as a fluorescent cholesterol reporter molecule.

Chapter 3 describes findings indicating that the behavior of the enantiomer of cholesterol does not differ from that of the parent molecule in monolayers and multilamellar vesicles.

Under conditions of cellular stress, cholesterol is often oxidized to produce various oxygen-containing sterol species (*16*). The origin of the toxicity of these "oxysterols" is not clear (*17*). Chapter 4 represents an analysis of the molecular interactions of several oxidized sterols with a glycerophospholipid and

sphingomyelin. The results suggest that the presence of an additional oxygen atom (as a hydroxy or carbonyl group) alters the ability of the sterol to establish the tight associations necessary for formation of a liquid-ordered phase. The implications of these findings for the existence of detergent-resistant domains are discussed.

Lysophosphatidic acid (LPA) is the subject of Chapters 5 and 6. In Chapter 5, the interactions of this pleiotropic molecule with the lipid-binding domain of the actin-severing protein gelsolin are investigated using isothermal titration calorimetry (ITC). This technique relies on heat changes associated with binding, and has the advantage of being able to provide thermodynamic parameters of biomolecular interactions without the use of an exogenous probe. The results are discussed as they relate to the function of gelsolin as a lipid-binding serum protein. The affinity of the peptide for lipopolysaccharide (LPS) and LPA are compared.

In a continuation of the study of some of the properties of LPA, we applied ITC to estimate its critical micelle concentration (CMC) in water and in buffer containing various concentrations of sodium chloride, and the published results (*18*) are discussed in Chapter 6. The effects of acyl chain structure and salt concentration on the CMC of LPA were demonstrated to be significant, but the CMC of a lysosphingomyelin (sphingosylphosphorylcholine) was insensitive to the presence of sodium chloride.

The results presented in this thesis demonstrate how a small number of biophysical assays can be brought to bear on some well-defined problems within the vast realm of lipidomics, and how these methods can be used to obtain useful information about this broad topic.

Chapter 2

Comparison of the Physical Properties of Two Types of Cholesterol Probes, 6-Photo-cholesterol and BODIPY-Cholesterol, to the Native Compound in Model Membranes

Preface

The functions of cholesterol in mammalian cellular membranes have been the subject of intensive study over many decades. The interactions of cholesterol with glycerophospholipids (*19*) and sphingomyelin (*20, 21*) are essential for many cellular processes (*19*). The presence of cholesterol in the target membrane is required for the fusion of Semliki Forest virus (SFV) and Sindbis virus (SIN) and for the activity of the family of thiol-activated pore-forming toxins (*22*); thus, cholesterol can be considered a non-protein membrane "receptor" (*23-28*). High local concentrations of cholesterol are required for the formation of lipid microdomains or "rafts," which are believed to act as protein-localizing platforms; such domains have been implicated in the cellular trafficking and sorting of lipids and proteins (*29, 30*).

The activities of cholesterol in vivo and in vitro are highly structure-dependent. The 3β-hydroxy group, which anchors the sterol normal to the plane of the membrane, the rigid sterol ring system, and the nonpolar isooctyl side chain are essential for strong sterol-lipid interactions (*19, 24, 31*).

A common strategy that is used to increase our understanding of cholesterol-phospholipid interactions is to use analogs of cholesterol that contain a fluorophore or

another reporter group. The usefulness of a molecular probe depends on how well it mimics the parent compound. This chapter presents an analysis of the behavior of cholesterol analogs bearing a photoreactive group or a fluorophore in model membranes.

Part 1

A Photoactivatable Cholesterol Analog: 6-Photocholesterol

Introduction

Photolabeling has been used frequently to label lipid-binding proteins (*32, 33*). The technique requires chemical modification of the lipid of interest by the addition of a photoactivatable moiety (e.g., a diazirine, nitrene, or benzophenone functionality). On irradiation of the photoreactive ligand at the appropriate wavelength, a highly reactive species is produced, which cross-links covalently with a neighboring molecule (e.g., amino acid residues of a protein). The resulting cross-linked species can then be characterized by radio-analytical (if a radioactive atom such as ^{3}H, ^{14}C, ^{32}P, or ^{125}I is incorporated into the probe) or by mass spectral methods.

A photoactivatable analog of cholesterol (6-photocholesterol, Figure 1), in which the C5,C6 double bond is removed and replaced by a diazirine functionality (a carbene precursor) at C6, has been used to successfully photolabel a cholesterol-binding protein in *Caenorhabditis elegans* (*34*), to study the interactions of cholesterol with proteolipids in oligodentrocytes (*35*), to identify a glutamate receptor in *Drosophila melanogaster* (*36*), and to label the cholesterol-binding domain in human metastatic lymph node 64 (*37*).

To determine whether 6-photocholesterol differs appreciably from native cholesterol in model membranes, we employed the monolayer technique to observe the compression of (a) pure sterol monolayers and (b) binary films of sterol and 1-palmitoyl-2-oleoyl-s*n*-3-phosphocholine (POPC). The results were compared with the properties of cholesterol in monolayers with POPC (*38, 39*). Additional experiments were performed by Barry-Lee Waarts in the laboratory of Dr. Jan Wilschut (Department of Medical Microbiology, Molecular Virology Section, University of Groningen, Groningen, The Netherlands) to compare the ability of 6-photocholesterol vs. cholesterol to mediate low pH membrane fusion using a pyrene excimer quenching assay in two viral systems, as described below.

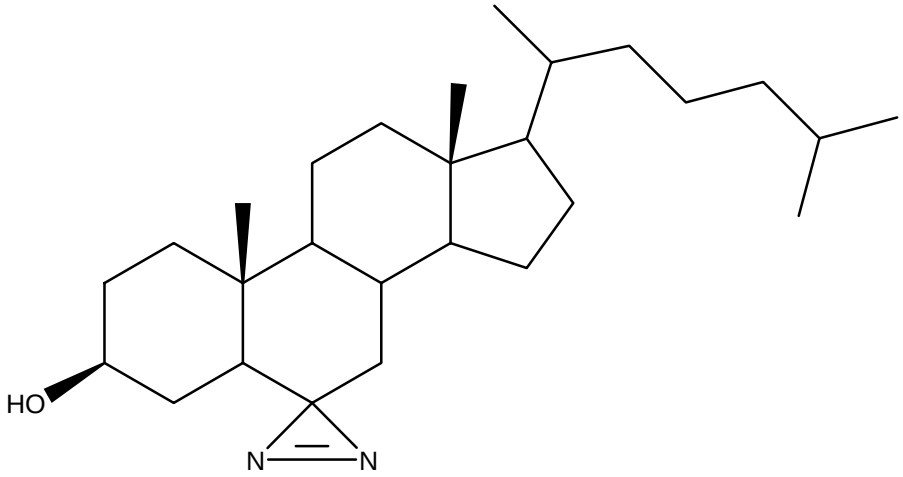

Figure 1. 6-Photocholesterol

Materials and Methods

Cholesterol and POPC were purchased from Avanti Polar Lipids (Alabaster, AL) and were used without further purification. 6-Photocholesterol was synthesized from 6-keto-5α-cholesten-3β-ol by Dr. Kochurani Jacob as described in (*35*).

Monolayer experiments were performed on a computer-controlled Kibron μ Trough S surface balance (Helsinki, Finland). Pre-weighed dry lipids were dissolved in a spreading solvent of HPLC-grade hexane/2-PrOH (3:2) to a concentration of ~1 mg/ml, stored at -20 °C, and warmed to room temperature before use. Experiments were conducted at ambient temperature (~21 ± 1°C). All glassware was acid-washed. Binary mixtures were produced by adding appropriate volumes of lipid stock solutions immediately prior to each experiment. Films were produced on a subphase of pure water (distilled and passed through a Milli-Q (Millipore Corp., Bedford, MA) water purification system to a resistivity of 18 MΩ·cm) by applying a small aliquot (<10 μl) of lipid-containing solvent from a digital Hamilton syringe to the surface of the subphase. The syringe was rinsed repeatedly with the spreading solvent, and the trough was cleaned with water and MeOH between experiments. Compressions of lipid films at a rate not exceeding 4 $Å^2$/molecule/min were initiated after allowing time for the solvent to evaporate (~ 5 min). Experiments with 6-photocholesterol were conducted in the dark in order to avoid carbene formation and subsequent cross-linking.

Compression data were collected with proprietary software from Kibron (Filmware) and were analyzed using Filmfit software (Creative Tensions, Austin, MN). Equation 1 describes ideal additivity of a binary film,

$$A_\pi = X_1(A_1)_\pi + (1-X_1)(A_2)\pi \qquad \text{Eq. 1}$$

where X_1 and $(1-X_1)$ are the mole fractions of components 1 and 2, respectively, and $(A_1)_\pi$ and $(A_2)_\pi$ are the molecular areas of pure components 1 and 2 at identical

surface pressure, π (*38*). Condensation results in negative deviations from the linear relationship described by Eq. 1, implying positive intermolecular attractions among the components comprising the film (*38*).

Results

Compression isotherms of pure 6-photocholesterol and of cholesterol are shown in Figure 2. The average molecular area occupied by 6-photocholesterol (curve b) is about 1-2 $Å^2$ greater than that of cholesterol (curve a) at surface pressures up to about 20 mN/m. The presence of the diazirine functionality slightly attenuates the sharp increase in pressure that occurs in its absence; this is probably the result of a tilt in the molecule relative to the surface of the water. As the lateral pressure is increased, the steep rise in pressure present in cholesterol's isotherm is evident. Agreement between the collapse pressures of the two molecules (46.1 ± 0.2 mN/m) indicates that both sterols can withstand similar lateral pressures.

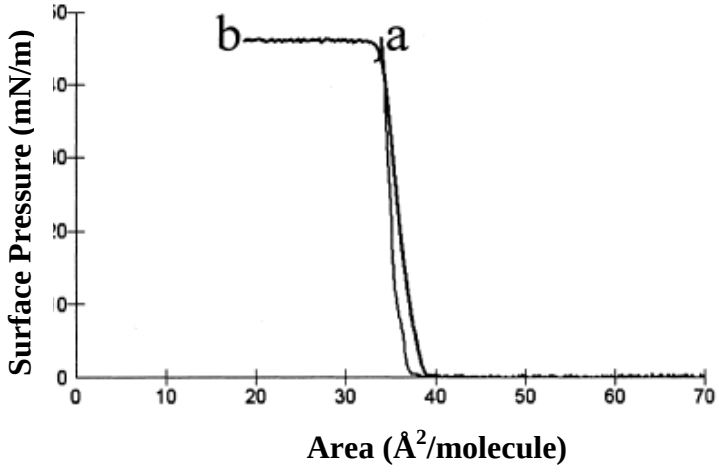

Figure 2. Force-area curves of pure cholesterol (*a*) and 6-photocholesterol (*b*) monolayers compressed on a pure water subphase. Isotherms were reproducible to ± 2 $Å^2$/molecule. Experimental details are described in *Materials and Methods.* (From (*15*).)

The well-known ability of cholesterol to increase the packing density of phospholipids (*39, 40*) presents a convenient method for comparison of sterols with respect to their interactions with POPC. To ascertain the extent to which 6-photocholesterol condenses POPC films compared with cholesterol, mixed films of the phospholipid and increasing mole fractions of either sterol were compressed at the air-water interface. Both compounds formed stable monolayers at all mole fractions examined (isotherms not shown). With either 6-photocholesterol or cholesterol, as the sterol mole fraction was increased the liquid-expanded phase of POPC began to condense to a liquid-ordered phase, and at 70 mole % sterol the films were completely condensed, indicating a high degree of ordering of the fatty acyl chains of POPC.

The ability of 6-photocholesterol to condense POPC was estimated by plotting the mean molecular areas of the mixtures as a function of composition at three surface pressures. The results, as well as the effect of cholesterol on POPC monolayers, are illustrated in Figure 3.

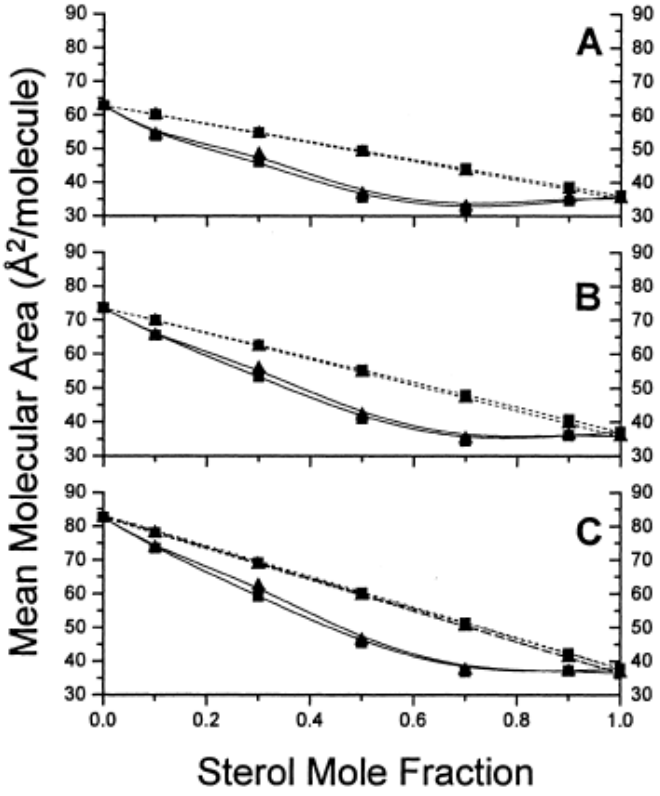

Figure 3. Area-composition curves for cholesterol (triangles) and 6-photocholesterol (squares) at 20 mN/m (*A*), 10 mN/m (*B*), and 5 mN/m (*C*). Dotted lines represent ideal additivity as described by Eq. 1. (From (*15*).)

The data show that intermolecular attractions between each sterol and POPC, as evidenced by negative deviation from ideality (represented by dashed lines), are significant for each composition at all surface pressures examined. The condensation effect of both sterols on POPC films was virtually identical.

An additional comparison of 6-photocholesterol and cholesterol was carried out using a viral fusion assay. This assay relies on the requirement for cholesterol in the target membrane of large unilamellar vesicles (LUVs) for the low pH-dependent fusion of SFV and SIN (*26-28, 41*). The extent of fusion is measured by a decrease in

excimer fluorescence resulting from dilution of pyrene-labeled viral lipids on fusion with LUVs. In the experiments conducted, efficient fusion of membranes occurred when the sterol in the target membrane was cholesterol or 6-photocholesterol[1]. Both sterols mediated fusion to similar degrees at the pH values investigated (Figure 4).

[1] The greater extent of fusion of SFV and SIN with LUVs containing 6-photocholesterol compared to those containing cholesterol is explained by the ability of 6-photocholesterol to quench monomer and excimer pyrene fluorescence. Importantly, the pH threshold is nearly identical for LUVs comprised of either sterol (Figure 4; see Ref. 22.)

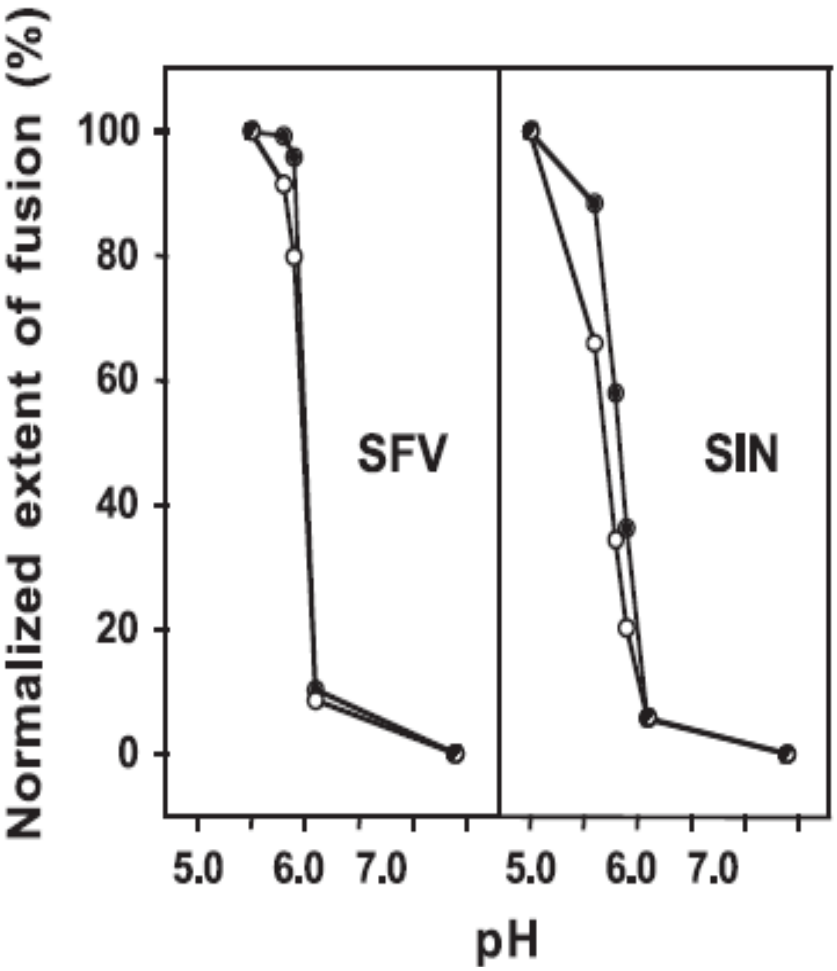

Figure 4. Results from acid pH-mediated viral fusion assay as measured by Dr. Jan Wilschut and Dr. Barry-Lee Waarts. A comparison of pH thresholds for SFV and SIN fusion with vesicles containing 6-photocholesterol (solid circles) or cholesterol (open circles) illustrates similar properties for both sterols. (From (*15*).)

Discussion

The goal of this project was to use a well-established biophysical technique to determine the ability of 6-photocholesterol, a photoactivatable analog of cholesterol, to mimic the behavior of the parent molecule in model membranes. This photoprobe has been used to identify several cholesterol-binding proteins (*34-37, 42*), as has another structurally similar analog, 7-photocholesterol, in which the photoreactive diazirine group resides at C7 (*43, 44*). 7-Photocholesterol supported the growth of cholesterol-requiring mutant cell lines, indicating that this probe also has the ability to mimic cholesterol (*44*). The experiments described in this chapter were carried out to determine whether a chemical modification, in this case the replacement of the C5,C6 double bond with a C6 diazirine functionality, results in a significant perturbation of the properties of the sterol.

The monolayer approach is a convenient and ideally suited method for such studies (*45, 46*). Increased fatty acyl chain ordering of phospholipids in the presence of cholesterol, which results from a reduction of trans-gauche isomerization, decreases the apparent molecular area of binary films relative to that occupied by the pure lipids (*47*), and represents a measure of the affinity of a phospholipid with the sterol.

Cholesterol's structure directly influences its membrane behavior. The 3β-hydroxy group anchors the sterol to the interface, the rigid sterol nucleus stabilizes the acyl chains, and the non-polar isooctyl side chain contributes to the van der Waals forces between neighboring lipids (*48-50*). With such a high degree of correlation

between structure and function, it would not be surprising if 6-photocholesterol differed from cholesterol in terms of biophysical properties.

The results reported in this chapter suggest that this probe is suitable for in vitro studies of cholesterol's interactions in membranes. The replacement of the C5,C6 double bond with the diazirine group did not disturb the tight lipid packing required to condense POPC monolayer films (Figure 3). (Previous studies have shown that dihydrocholesterol, which also lacks the C5,C6 double bond, behaves similarly to cholesterol in monolayer and other assays (*51, 52*).) Support for this conclusion is provided by the viral fusion data (Figure 4), which demonstrate the ability of 6-photocholesterol to efficiently mediate SFV and SIN fusion with probe-containing LUVs.

Part 2

BODIPY-Cholesterol: A New Fluorescent Analog of Free Cholesterol

Introduction

Conjugates of a fluorophore with biological molecules to produce molecular probes are widely used to probe the properties of the unconjugated biomolecule. Molecular distance relationships, cellular transport, protein folding, and membrane dynamics are examples of phenomena that have been studied with fluorophore-containing probes (*14, 53-55*). Borondipyrromethene (4,4-difluoro-4-bora-3a,4a-diaza-*s*-indacenes, BODIPY) is used extensively because of its attractive spectral properties (*56*) and relatively small size. DNA, proteins, carbohydrates, and lipids have been modified with BODIPY to produce fluorescent analogs (*57-59*).

The incorporation of the BODIPY moiety into free (unesterified) cholesterol may provide a useful probe for membrane studies. Until now, the BODIPY fluorophore has only been conjugated to cholesterol via an ester linkage at the C3 position, thus affording a fluorescent analog of a cholesteryl ester. The synthetic challenges associated with attaching the hydrophobic BODIPY group at the nonpolar sterol side chain, where there are no functional groups, have recently been overcome by Dr. Zaiguo Li and Professor Robert Bittman, producing the first BODIPY analogs of free cholesterol (Figure 1).

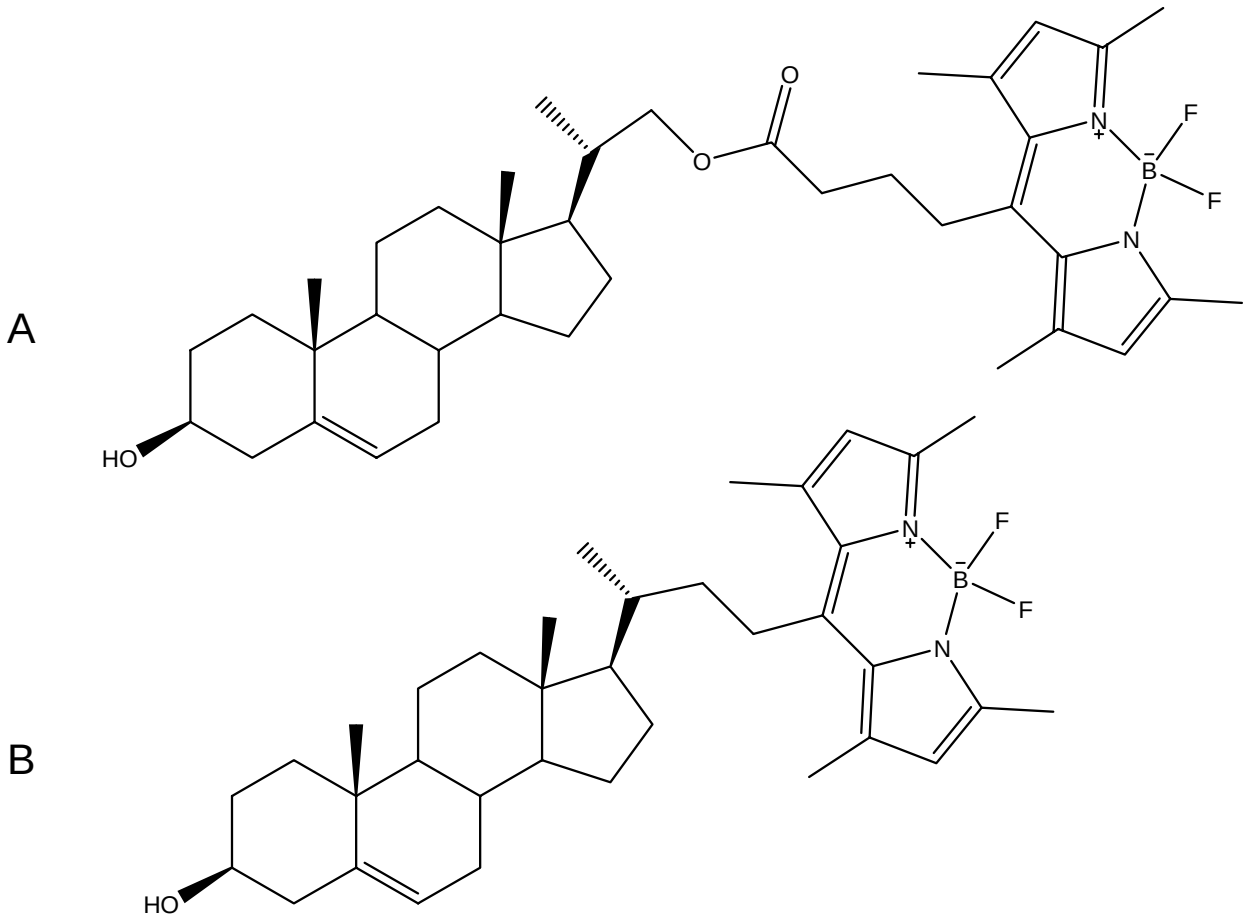

Figure 1. Synthetic cholesterol analogs. A, BODIPY-cholesterol analog **1** (CPD-1); B, BODIPY-cholesterol analog **2** (CPD-2).

These two BODIPY-containing cholesterol analogs differ in the linkage of the fluorophore to the sterol. Both are attached to the aliphatic side chain, but BODIPY-cholesterol analog **1** (CPD-1) contains an ester linker, whereas BODIPY-cholesterol analog **2** (CPD-2) is devoid of oxygen atoms in the side chain.

As in Part 1 of this chapter, the mixed monomolecular film method was employed to compare the behavior of both analogs to that of cholesterol. Monolayers of CPD-1 and CPD-2 and POPC were compressed at the air-water interface, and the condensation effect of each of these probes was analyzed. The properties of these probes were also investigated by examining the kinetics of cyclodextrin-mediated desorption from mixed monolayers comprised of POPC and sterol, an assay that relies on the ability of cyclodextrins to remove cholesterol from monolayers and membranes and is a measure of intermolecular forces between lipids (*60*). Finally, a detergent-solubility assay was used to ascertain the propensity of the probes to form insoluble liquid-ordered domains in multilamellar vesicles (MLVs). In addition, Megha in the laboratory of Prof. Erwin London (Department of Biochemistry and Cell Biology, Stony Brook University, State University of New York, Stony Brook, NY) examined the ability of the probes to partition into liquid-ordered domains in MLVs using a fluorescence assay.

Materials and Methods

Monolayers

Monolayer experiments were conducted as described in the *Materials and Methods* section of Part 1.

Detergent solubility assay

The extent of detergent solubility was determined by treatment of MLVs, comprised of milk sphingomyelin (MSPM) (Avanti Polar Lipids, Alabaster, AL) and

sterol, with Triton X-100 (Sigma-Aldrich, St. Louis, MO) essentially as described in (*61*). Briefly, appropriate volumes of sterol and MSPM stock solutions in $CHCl_3$/MeOH (2:1) were combined to produce mixtures of varying mol ratios (total lipid: 500 nmol). MLVs were prepared by evaporating the solvent under a gentle stream of nitrogen, drying the resulting films under vacuum overnight, then hydrating with 1.6 ml of hot PBS (~ 85° C). The suspensions were vortexed vigorously for 60 s, incubated at high temperature for 30 min, re-vortexed for 60s, and allowed to cool to room temperature (23 ± 1° C). The optical density (OD) was measured at 600 nm in an OOIBase32 spectrophotometer (Dunedin, FL) before and ~24 h after addition of 40 µl 10% (w/v) Triton X-100. The % OD remaining after detergent treatment was calculated using Eq. 2 (*62*):

$$\%\ OD_{600}\ \text{remaining} = OD_{600}\ (+\ \text{detergent}) / OD_{600}\ (-\text{detergent}) \times 100 \qquad \text{Eq. 2}$$

Cyclodextrin-mediated desorption from monolayers

Lipid mixtures comprised of POPC and 33 mol % of either cholesterol or CPD-2 were applied to the air-water interface, using a circular Teflon trough (volume ~14 ml), to give initial surface pressures between 25 and 30 mN/m. After a stable monolayer was obtained, as indicated by constant surface pressure (between 15 and 20 mN/m), 200-µl aliquots of 2-hydroxypropyl-β-cyclodextrin (HPCD) (Cerestar, Hammond, IN), dissolved in pure water, were injected into the stirred subphase through a side port of the trough (final concentration, 3 mM) without puncturing the lipid film. Control experiments in which a solution of HPCD was injected under a

pure POPC monolayer did not produce a significant change in the surface pressure. The HPCD-induced desorption of sterol from the binary film was monitored by the decrease in surface pressure. The first-order rate constant was calculated from the slope of the best-fit line through the data plotted according to Eq. 3:

$$\log (\pi_t - \pi_{infinity}) = -kt/2.303 \qquad \text{Eq. 3}$$

where $(\pi_t - \pi_{infinity})$ is the difference between surface pressures at time t and after equilibrium has been reached and k is the first-order rate constant.

Results

Pure sterol monolayers

The compressions of monolayers formed from CPD-1 and CPD-2 at the air-water interface are compared with that of cholesterol in Figure 2. The 3β-hydroxy group of these molecules anchors them to the surface. The rigid sterol ring system causes an abrupt rise in pressure as the lateral pressure is increased. The very steep rise in the cholesterol isotherm (curve a) is indicative of an orientation normal to the plane of the interface (*63, 64*). The compression curves for CPD-1 and CPD-2 (curves b and c, respectively) are less steep, indicative of a higher degree of tilt of these molecules relative to the surface of the subphase. The analogs occupy a significantly larger area than cholesterol at surface pressures below ~30 mN/m. CPD-1, which contains an ester linkage in the aliphatic tail, occupies a larger area than CPD-2 as the lateral pressure increases.

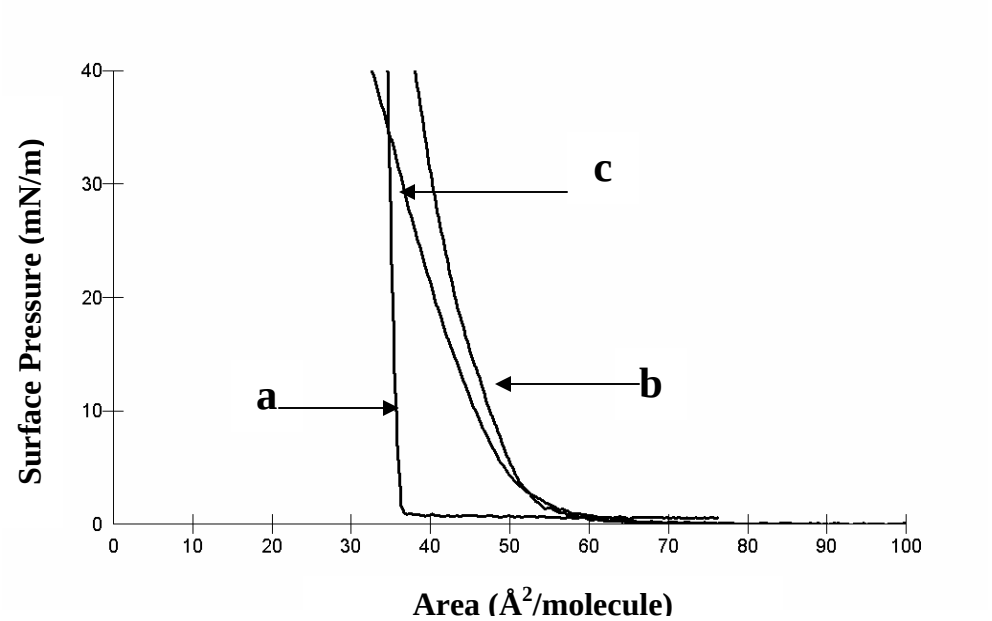

Figure 2. Compression isotherms of cholesterol (*a*), CPD-1 (*b*), and CPD-2 (*c*). Compressions were performed on a subphase of pure water as described in the *Materials and Methods* section of Part 1 of this chapter. Errors were ± 2 $Å^2$/molecule.

Mixing behavior in two-component monomolecular lipid films

The molecular areas of mixed monolayers comprised of varying mole fractions of sterol and POPC at three surface pressures are shown in Figure 3. The straight lines represent the areas expected from ideal mixing of the two components. The smaller area of cholesterol-POPC films (squares) illustrates the well-known condensation effect of cholesterol, which is considered to arise because intermolecular interactions result in a reduced number of gauche conformers in the phospholipid's fatty acyl chains (*65*). The positive deviation from ideal mixing observed with CPD-1 is indicative of demixing of the POPC-sterol film (triangles). Demixing is presumably a consequence of the oxygen atoms in the ester linkage used

to conjugate the sterol with the BODIPY moiety. CPD-2, in which there are no polar atoms in the linker between the sterol side chain and the fluorophore, mixes in an ideal manner with POPC at the surface pressures and mole fractions we examined (circles). However, unlike cholesterol, CPD-2 did not induce condensation of the molecular area of POPC at the surface pressures we examined, and thus is not a perfect cholesterol mimetic.

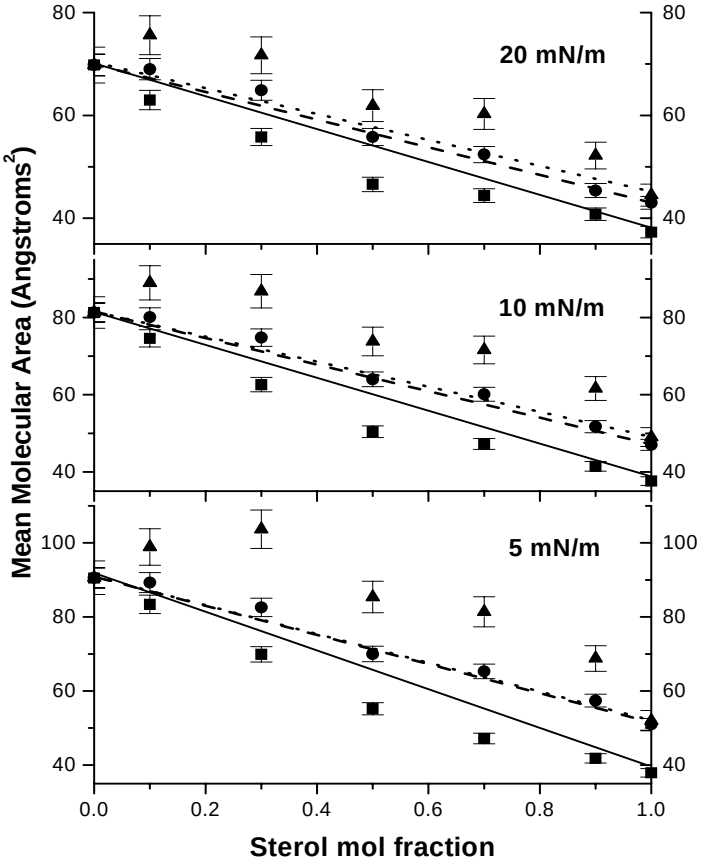

Figure 3. Area-composition curves for cholesterol (squares), CPD-1 (triangles), and CPD-2 (circles) at three surface pressures as labeled. Solid, dotted and dashed lines represent ideal additivity of cholesterol, CPD-1, and CPD-2, respectively, as described by Eq. 1, Part 1 of this chapter. (Note: Although the absolute area of

cholesterol appears larger than that shown in Figure 3 of Part 1 (p. 11), the condensation effects, as represented by changes in molecular area in the presence of POPC, are comparable.)

Detergent-solubility assay

To examine the interactions between CPD-2 and phospholipids in more detail, we compared the ability of cholesterol and this analog to support lipid domain formation in bilayer membranes. The method employed relies on the well-known ability of MLVs comprised of mixtures of saturated phospho-or sphingolipids and sterols to form detergent-resistant domains (*62, 66*). This property is sensitive to sterol structure (*62, 67*). As shown in Figure 4, the interactions between the sterols and MSPM, as indicated by the ability to support raft formation, were within experimental error at the molar ratios examined. These results suggest that the BODIPY moiety in CPD-2 does not interfere with the tight lipid packing required for formation of lipid raft domains in MLVs. Comparable results were observed when similar experiments were conducted by Mehga in Prof. London's laboratory. It was also found that CPD-1 did not partition as well as cholesterol into the insoluble fraction of detergent-treated MLVs as determined by the ratio of fluorescence intensity of the pellet compared to that of the supernatant after centrifugation. It should be noted, however, that bath sonication of the MLVs was required to disperse the lipids; therefore, the results are qualitative.

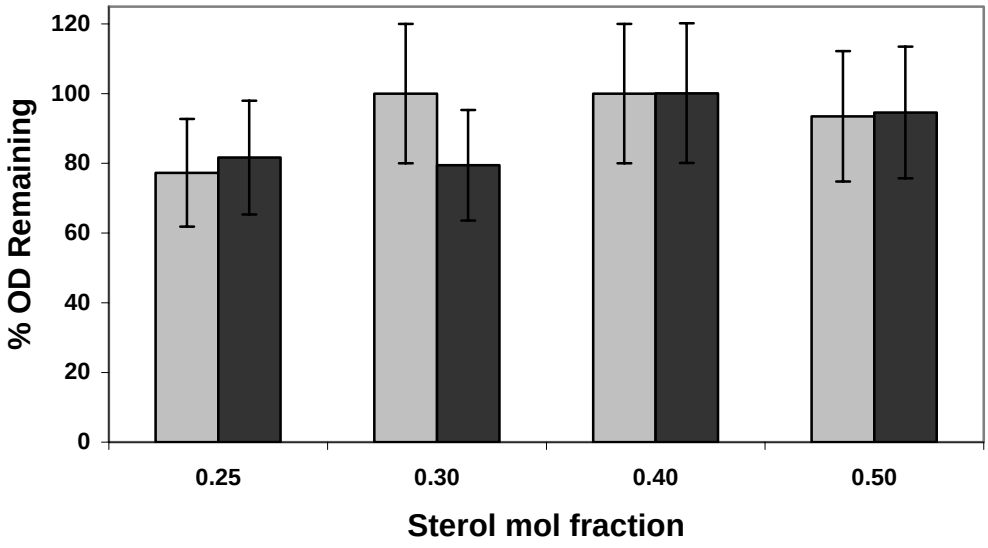

Figure 4. Plot of % OD remaining at 600 nm and 23 ºC in MLVs composed of binary mixtures of MSPM and cholesterol (gray bars) or CPD-2 (dark bars). The total lipid concentration was 312 μM. MLVs were prepared and treated with Triton X-100 as described in *Materials and Methods*. The average and standard deviation of triplicate samples are shown.

Cyclodextrin-mediated adsorption from monolayers

The rates of desorption of cholesterol and CPD-2 from mixed monolayers composed of POPC and sterol at constant surface area on injection of a water-soluble cyclodextrin derivative into the subphase are shown in Figure 5. This method has been used to estimate the extent of interaction of sterols with phospholipids in monolayers (*60*). Figure 5 shows that the kinetics of HPCD-induced desorption of cholesterol and CPD-2 from the monolayers are similar, based on the calculated first-order rate constants. These results suggest a similar affinity of the sterols for POPC under the conditions employed. No decrease in surface pressure was observed in

control experiments in which HPCD was injected into a monolayer devoid of cholesterol or CPD-2 (data not shown).

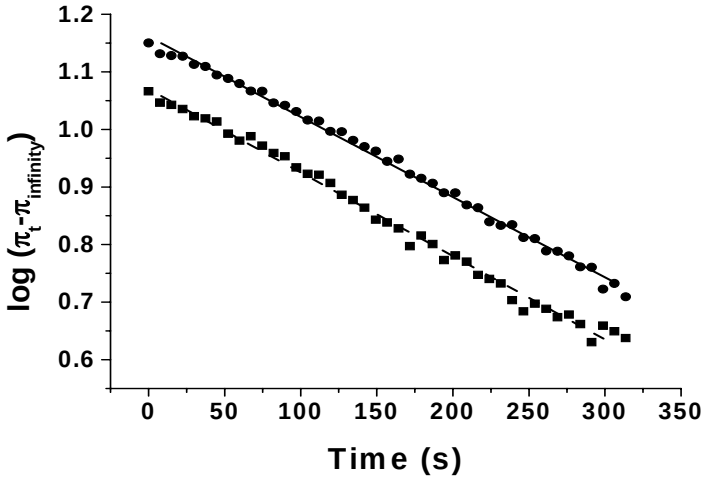

Figure. 5. First-order kinetic plot of sterol displacement from POPC/sterol monolayers on injection of HP-CD into the subphase at 23 ºC. HP-CD was injected into the subphase at a final concentration of 3 mM. The data were fit with first-order rate constants of 3.3 x 10^{-3} s^{-1} for cholesterol (squares) and 3.2 x 10^{-3} s^{-1} for CPD-2 (circles). The molar ratio of POPC/sterol was 2:1.

Discussion

Our understanding of membrane dynamics has been increased by the use of fluorescent lipid analogs (*68-70*). Several fluorescent cholesterol analogs have been used, but many have proven to be problematic with respect to faithfully mimicking the membrane behavior of the natural compound. The site of attachment of the fluorophore to the sterol molecule and the size and physical properties of the fluorophore may affect how the probe molecule is partitioned in membrane domains.

For example, a nitrobenzoxadiazole (NBD) moiety has been conjugated to cholesterol at C22 and C25 (*71*). However, unlike cholesterol, whose side chain is deeply imbedded among the fatty acyl groups of phospholipids in the non-polar interior of the membrane (*19*), these probes tend to be oriented (at least transiently) with their side chain near the polar milieu, as evidenced by the quenching of fluorescence by the water-soluble compound dithionite (*72*), and the probe with the NBD group at C22 was also shown to distribute preferentially into the liquid-disordered phase, unlike cholesterol under similar conditions (*73*). A cholesterol analog in which a dansyl group was coupled to cholestanol at C6 was used to study cholesterol transport, and this probe was reported to mimic cholesterol with respect to supporting raft formation and efflux by cyclodextrin from cells (*52*). However, it must be noted that this fluorophore is more hydrophilic than BODIPY and, when attached to various sites on phosphatidylethanolamine, was shown to localize with the polar head groups of neighboring lipids near the aqueous phase (*74*). This property may cause differences in the membrane orientation that the probe adopts compared to cholesterol. These findings indicate that NBD- and dansyl-cholesterol may not be suitable probes for cholesterol.

Fluorescent analogs of cholesterol without large functional groups are available (e.g., cholestatrienol and dehydroergosterol), but they possess some undesirable spectroscopic properties (low quantum yield, excitation wavelengths in the UV). Therefore, they are not appropriate reporter molecules for live cell imaging studies.

In light of the limitations of the fluorophores discussed above, it can be concluded that BODIPY cholesterol is a more promising reporter molecule for studies of membrane dynamics in which the sterol is involved. CPD-2 exhibits similar behavior to cholesterol, based on the results from the cyclodextrin desorption and detergent solubility assays reported here. Furthermore, CPD-2 mixes in an ideal manner with POPC (Figure 3), although it fails to induce POPC condensation in monolayer films. Therefore, CPD-2 has the potential to act as a faithful analog in model membrane and cell studies. On the other hand, CPD-1, which displays non-mixing properties in POPC monolayers, may have utility as a probe that tends to partition into non-raft domains.

Summary

The experiments described in Parts 1 and 2 of this chapter were directed at ascertaining the degree to which two types of cholesterol analogs mimic the biophysical behavior of the parent compound in model membrane systems. A photoactivatable analog, 6-photocholesterol, in which the C5,C6 double bond is absent and a carbene precursor is installed at C6, displayed a compression isotherm that differed from that of cholesterol by only ~1.5 $Å^2$ at lift-off area. The collapse pressure and area were almost identical to those of cholesterol, and its ability to condense POPC was essentially indistinguishable to that of cholesterol.

The behavior of two cholesterol analogs containing a BODIPY fluorophore linked to the side chain was also examined. The ester linker in CPD-1 appears to interfere with lipid packing in monolayers. On the other hand, CPD-2 interacted

quite similarly to cholesterol with POPC and MSPM in two additional assays. Thus, it can be concluded that these probes can be used in tandem, one as a cholesterol analog and one as a negative control, to study membrane dynamics involving cholesterol, with a greater measure of confidence than several other, widely used fluorescent cholesterol conjugates.

Chapter 3

Cholesterol-Phospholipid Interactions in Monolayers and Multilamellar Vesicles Are Not Enantiospecific

Abstract

Compressions of monomolecular films comprised of 1-palmitoyl-2-oleoyl-*sn*-glycero-3-phosphocholine (POPC) and cholesterol or its enantiomer (ent-cholesterol) were performed at the air-water interface. There is no significant difference between the interactions of POPC with cholesterol or ent-cholesterol under the conditions employed. The ability of ent-cholesterol to form lipid-ordered domains in multilamellar vesicles with egg sphingomyelin was similar to that of cholesterol. These results suggest that sterol-phospholipid interactions in model membranes are not enantiospecific with respect to the sterol molecule.

Introduction

The importance of cholesterol structure for function in vitro and in vivo is well established (Chapters 2 and 3 of this thesis, (*19, 60, 67, 75*)) but evidence for enantiospecificity of lipids or peptides for cholesterol has been sought for some time (*76-78*). The total synthesis of a cholesterol analog in which every stereocenter is reversed (Figure 1) (*79, 80*) presents an opportunity to study the enantiomer of the natural sterol molecule and compare its biological and biophysical behavior to that of natural cholesterol.

Replacement of cholesterol with ent-cholesterol in *C. elegans* had only minor effects on first generation animals, but later generations were nonviable (*76*), indicating that the enantiomer displayed lethal differences in function in vivo. In recent in vitro experiments, an ordered-domain forming peptide had differential effects on phase transition properties in liposomes containing ent-cholesterol or cholesterol and 1-stearoyl-2-oleoyl-*sn*-glycero-3-phosphocholine (SOPC) (*81*). Another investigation revealed enantiospecific sterol-protein interactions but no such specificity with respect to sterol-phospholipid interactions (*82*). However, several other recent in vitro studies failed to detect any specificity in various biophysical assays (*78, 83*). There are some studies that show small effects of cholesterol enantioselectivty. A comparison of the monolayer behavior and detergent solubility of ent-cholesterol and cholesterol in multilamellar vesicles (MLVs) is reported in this chapter.

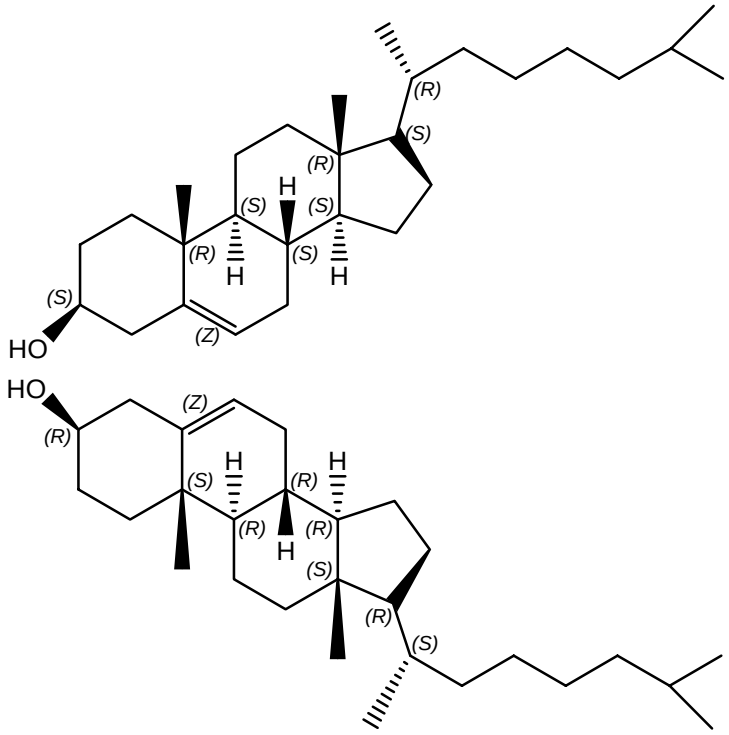

Figure 1. Structures of cholesterol (top) and ent-cholesterol (bottom) showing stereocenters.

Materials and Methods

POPC, ESPM, and cholesterol were purchased from Avanti Polar Lipids (Alabaster, AL). Ent-cholesterol was a generous gift from Prof. Douglas Covey (Washington University School of Medicine, St. Louis, MO). Isothermal compressions of pure sterol and mixed sterol-POPC monolayers and determination of the formation of liquid-ordered phases by measurement of optical density remaining after Triton X-100 (Sigma-Aldrich, St. Louis, MO) treatment of MLVs were performed as described in Chapters 2 and 3 of this thesis.

Results

The molecular area and collapse pressure of pure cholesterol and ent-cholesterol monolayers were similar (Figure 2). However, a less abrupt "lift-off" of ent-cholesterol compared to cholesterol was observed, which may be the result of a slight twist and less extended conformation in the enantiomeric molecule.

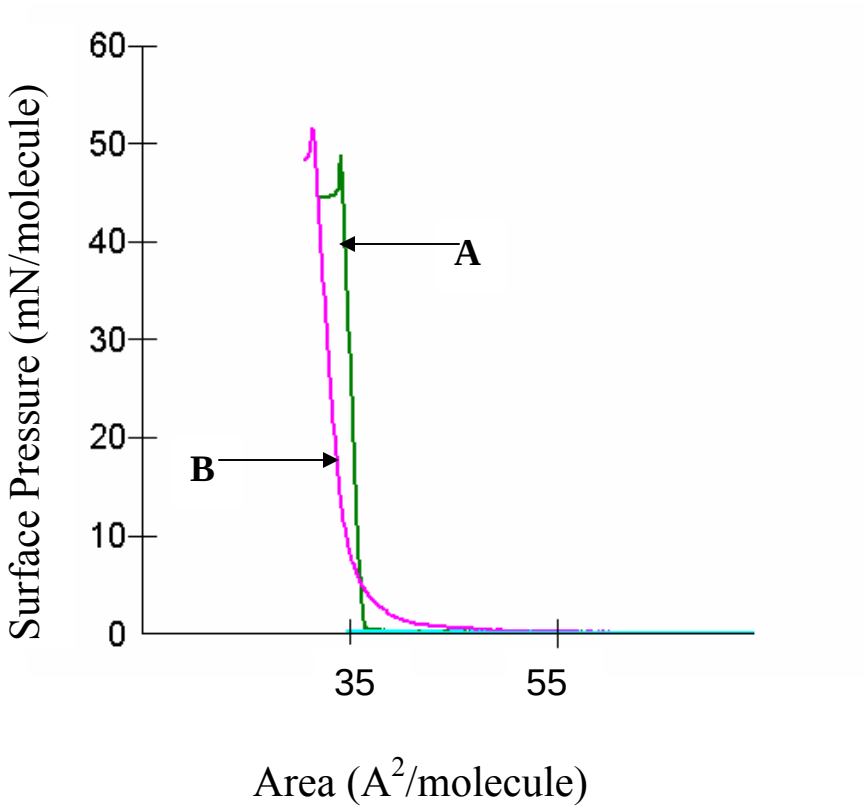

Figure 2. Compression isotherms of cholesterol (A) and ent-cholesterol (B) on a subphase of pure water at 22 °C. Isotherms shown are representative of 3-4 compressions and were reproducible to within 2 $Å^2$/molecule.

To investigate whether the complete reversal of stereochemistry affected sterol interactions with other membrane lipids, binary monolayer films comprised of

varying mol fractions of sterol and POPC were compressed at the air-water interface. As discussed in the preceding chapters, lipid-lipid interactions can be measured qualitatively by comparing the molecular area occupied by mixed monolayers to the area that would be occupied if the lipids mixed in an ideal manner. As Figure 3 illustrates, ent-cholesterol condensed POPC films to a similar extent as cholesterol at sterol mol fractions lower than 0.5. As the sterol mol fraction was increased, the effect of ent-cholesterol on POPC films was slightly decreased compared with cholesterol; the altered orientation the molecule appears to adopt, as suggested by the pure isotherms in Figure 2, may be responsible for this behavior.

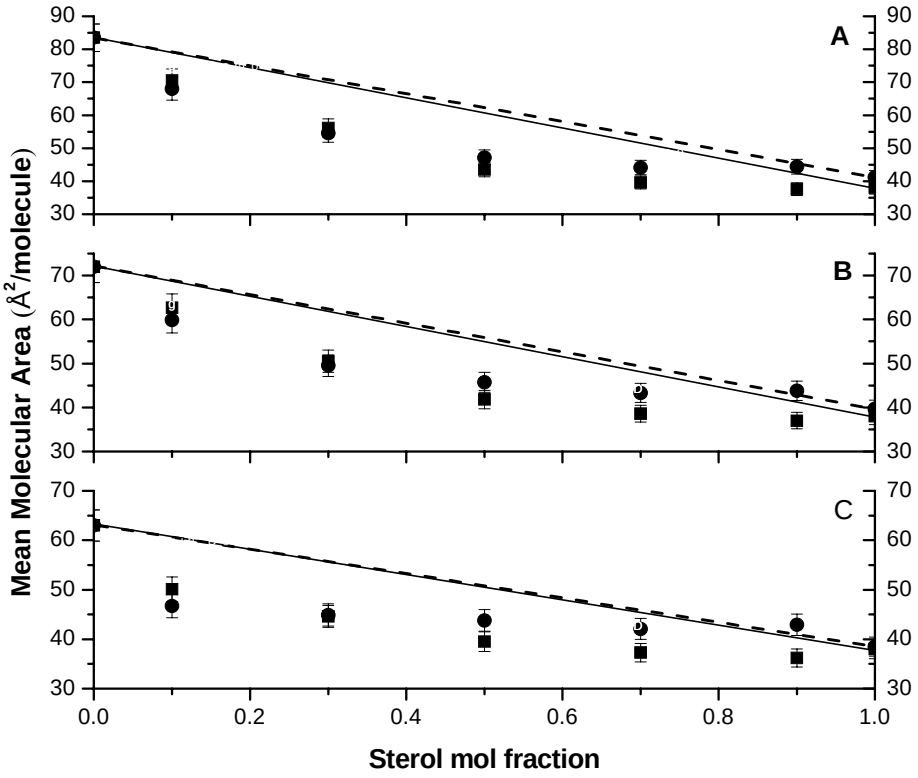

Figure 3. Area-composition curves for cholesterol (squares) and ent-chol (circles). Straight lines represent ideal additivity of cholesterol (solid lines) and ent-cholesterol (dashed lines) as described in Chapters 2 and 3. Measurements are displayed for surface pressures of 5, 10, and 20 mN/molecule (panels A-C, respectively).

The propensity of ent-cholesterol to promote the formation of detergent-resistant lipid domains in MLVs comprised of sterol and ESPM was examined and compared to that of cholesterol. As shown in Figure 4, reversal of all of the chiral centers in cholesterol does not significantly alter this property. All of the general structural features of cholesterol (the 3β-hydroxy group, rigid ring system, and

aliphatic side chain) are intact in ent-chol, so that the molecular features required for tight sterol-sphingolipid interactions are maintained.

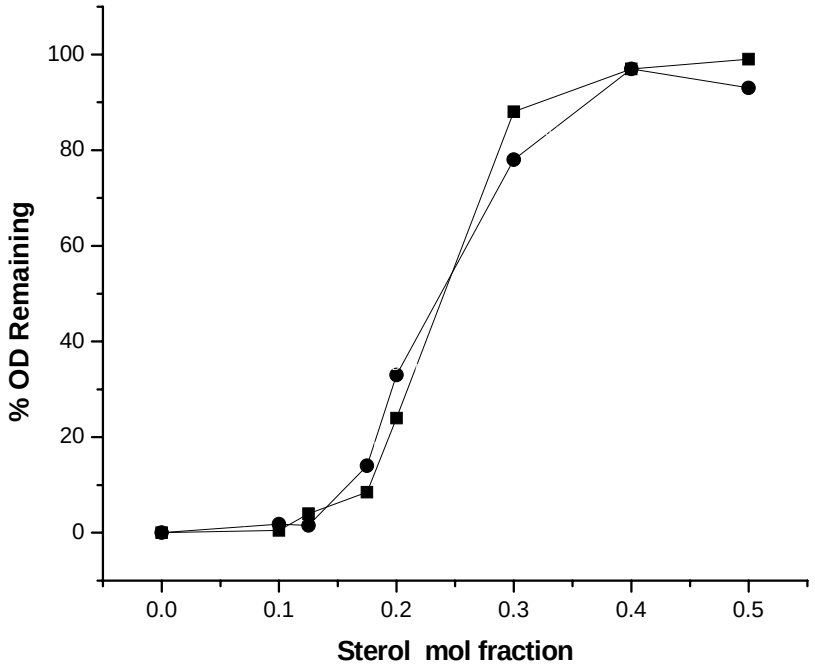

Figure 4. OD at 600 nm remaining after treatment of MLVs prepared from cholesterol (squares) or ent-cholesterol (circles) and ESPM with Triton X-100 at 23 °C. See Materials and Methods in Chapter 2 for experimental details.

Discussion

The results of pure sterol and POPC-sterol monolayer compressions and detergent-solubility assays failed to detect significant differences between ent-cholesterol and the natural compound. This conclusion is in agreement with several recent studies. For example, an antibody raised against cholesterol monohydrate

displayed similar affinity for both enantiomers, although no interactions were observed between the antibody and epicholesterol, the diastereomer that contains a C3-hydroxy group in the α orientation (*78*). Likewise, differential-scanning calorimetric measurements of phase transition temperatures and enthalpy changes failed to detect differences between bilayers comprised of either enantiomer and ESPM (*83*).

On the other hand, the thermodynamic parameters of SOPC phase transitions were altered at certain sterol mol fractions in the presence of a small, ordered-domain-inducing peptide when cholesterol was replaced with ent-cholesterol (*81*). Differences between cholesterol and ent-cholesterol were also observed in the degree of condensation of ESPM films in previous monolayer experiments (*84*). In addition, although the activity of the cholesterol-requiring pore-forming toxin Streptolysin O was virtually insensitive to the complete reversal of stereochemistry as represented by ent-cholesterol, the activity of a related toxin, *Vibrio cholerae* cytolysin, was significantly reduced when cholesterol was replaced by the enantiomer in liposomes (*85*).

Insight into these apparent inconsistencies may be provided by recent work in which phosphorylation of the membrane receptor for epidermal growth factor (EGF) was shown to be insensitive to the absolute configuration of cholesterol; conversely, cholesterol oxidase oxidized cholesterol to a significantly greater extent than it did ent-cholesterol (*82*). This study also found that lipid raft forming ability was maintained when ent-cholesterol was substituted for natural cholesterol. The authors argued convincingly that EGF receptor phosphorylation, like raft formation, is

dependent on cholesterol's presence for structural (physical) reasons. However, as the interactions with cholesterol oxidase (*82*) and with a raft-promoting peptide (*81*) illustrate, a degree of sterol-protein and sterol-peptide enantiospecificity was observed.

In conclusion, there are discrepancies regarding the effect of reversing the complete stereochemistry of cholesterol. The chemical modification was lethal to second generation progeny in an animal model (*76*) and altered the pore-forming properties of a cholesterol-requiring toxin (*85*). However, experiments measuring the phase-transition thermodynamics should be considered inconclusive in that the effect observed depended on whether lipid mixtures contained sterol and ESPM on one hand (insensitive to sterol stereochemistry) (*83*) and SOPC and a raft-promoting peptide on the other (sensitive) (*81*).

The assays employed in this study did not detect a significant difference between cholesterol and ent-cholesterol. Because of the conflicting results reported here and in the literature, additional research is required to determine whether the apparent enantioselectivity seen in several of the studies cited are a function of the sensitivity of the specific assay employed or of the sterol function, and whether sterol interactions with proteins are enantiospecific, whereas sterol-phospholipid interactions are not.

Chapter 4

Effect of Oxygenated Sterols on the Promotion of Detergent-resistant Domains in Multilamellar Vesicles and Condensation of Phospholipids in Monolayers

Abstract

The lipid products of oxidative stress include several different oxygen-containing sterols. These sterols are cytotoxic but the exact mechanisms of cell injury remain unclear. An investigation of the ability of various oxidized sterols to interact with phospholipids and to support lipid raft formation in model membranes was carried out. It was found that the presence of an oxygen atom in addition to the one in the hydroxyl group at C3 of cholesterol changes significantly the sterol's ability to condense phospholipids monolayers and support lipid raft formation. A ketone group at C7 had a greater effect on membrane properties than at C6 compared to cholesterol, and ketone groups on the aliphatic side chain also perturbed sterol behavior in the assays employed. Monolayer and raft-formation properties were also sensitive to the exact location of the oxygen at the side chain.

Introduction

The existence of cholesterol- and glycosphingolipid-rich membrane microdomains has been proposed since at least the 1980's (*86*). These domains have been termed "rafts;" detergent-insoluble, glycosphingolipid-enriched membranes;

cholesterol-enriched domains; and detergent-resistant membranes (DRM). The term DRM arises from the inability of these domains to be readily dissolved in Triton X-100 or other detergents. Lipid rafts have been implicated in a myriad of cellular functions, including protein trafficking, viral budding and infection, and various cell signaling activities (*87-90*). Many intrinsic proteins have been found in lipid rafts, including caveolins, glycosylphosphatidylinositol-(GPI) linked proteins (*91*), and cell signaling and sorting proteins (*87, 88*). Rafts are enriched in glycosphingolipids and cholesterol (*92*). The relatively low buoyant density of these domains causes them to float at the top of a sucrose gradient. The large proportion of highly saturated glycosphingolipids found in DRM suggests that lipids in the liquid-ordered (L_o) phase promote domain formation (*66*).

The presence of cholesterol mediates formation of the L_o phase (*93*), which has properties of both the liquid-crystalline (L_α) and gel (L_β) phases. Acyl chains in the L_o phase are extended and tightly packed like those in the gel phase, but they display lateral movement consistent with lipids in the liquid-crystalline phase (*66, 94*).

Cholesterol has a high affinity for raft phospholipids such as sphingomyelin and saturated glycerophospholipids. The structural requirements for sterols to promote DRM have been investigated (*67, 75, 95*). These studies revealed a sensitivity to sterol structural features (degree of saturation, hydrophobicity, and isooctyl side chain structure) with respect to DRM promotion. The same sterol structural features are well known to affect interactions with neighboring lipids in cellular and model membranes (*19*).

Oxidized sterols are present in high concentrations in atherosclerotic plaques (*6*). Gaus et al. (*96*) showed that reverse cholesterol efflux was inhibited in the presence of 5-cholesten-3β-ol-7-one (7-ketocholesterol; Figure 1). This oxysterol is less efficient in causing membrane lipids to adopt the L_o phase compared to native cholesterol (*64, 97*), and high concentrations of 7-ketocholesterol, such as is present in atherosclerotic plaques, caused Ca^{2+} release, leading to apoptosis (*98*). This sterol and another product of oxidative stress, 5-cholesten-3β,19-diol (19-hydroxycholesterol), have been found in red blood sickle cells (*99*). Indeed, many oxysterols are thought to be more atherosclerotic than native cholesterol (*100*). This chapter describes the results from a systematic study, using two unrelated assays, of a number of oxidized cholesterol analogs (see Figure 1 for structures). The goal of this project was to compare the properties of these sterols to cholesterol with respect to their ability to (i) support the formation of DRM as detected by the optical density (OD) of egg sphingomyelin-sterol (ESPM) multilamellar vesicles (MLVs) after treatment with Triton X-100 and (ii) condense diacylphosphatidylcholine (PC) monolayers at the air-water interface.

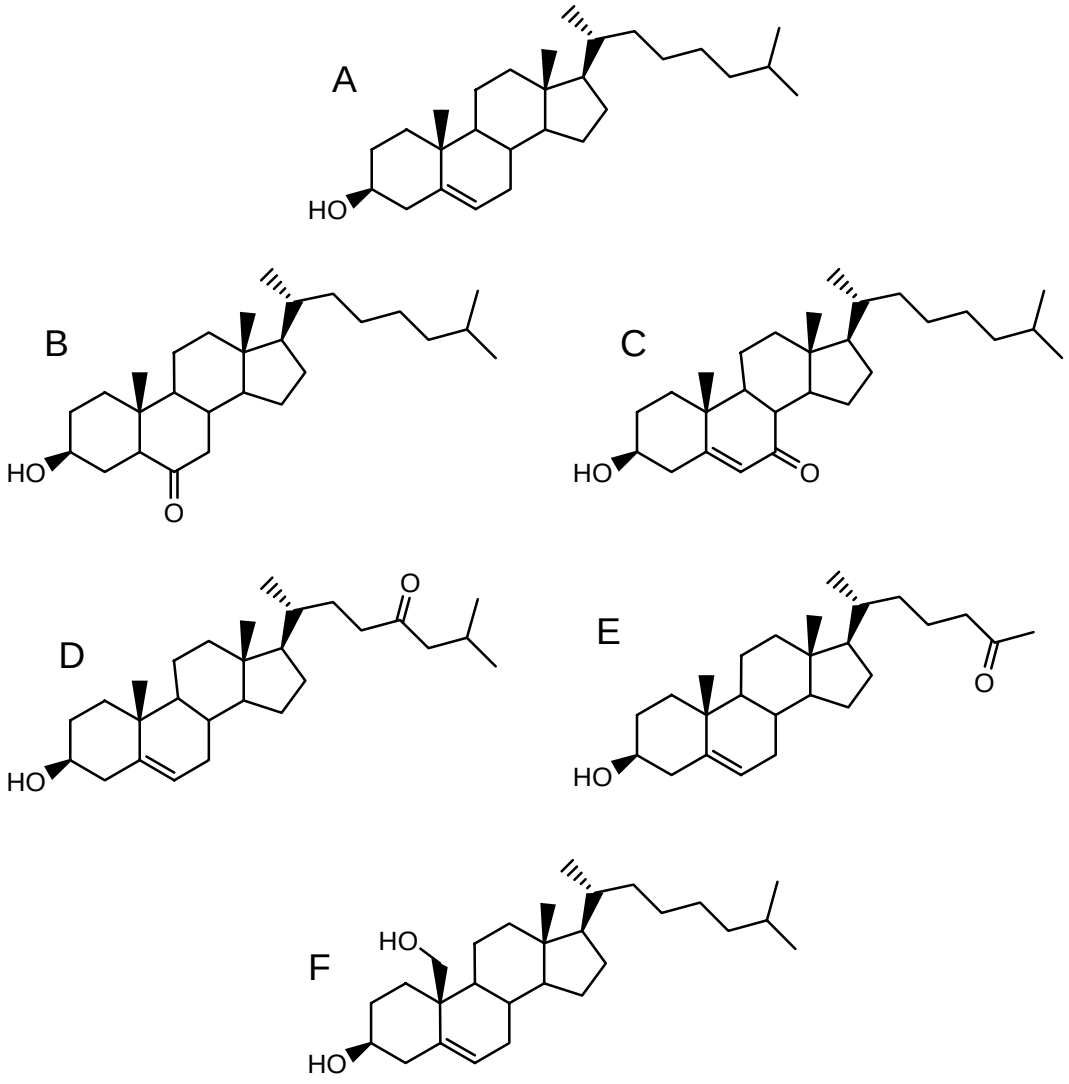

Figure 1. Structures of cholesterol (A) and oxygenated derivatives. B, 5-α-cholestan-3β-ol-6-one (6-ketocholesterol); C, 5-cholesten-3β-ol-7-one (7-ketocholesterol); D, 5-cholesten-3β-ol-24-one (24-ketocholesterol); E, 27-nor-5-cholesten-3β-ol-25-one (25-ketocholesterol); F, 5-cholesten-3β,19-diol (19-hydroxycholesterol).

Materials and Methods

1-Palmitoyl-2-oleoyl-PC and ESPM were from Avanti Polar Lipids (Alabaster, AL). Sterols were from Steraloids (Newport, RI) and Research Plus (Manasquan, NJ). Triton X-100 was from Sigma-Aldrich (St. Louis, MO).

MLVs were produced essentially as described by Li et al. (*61*) and in Chapter 2. Briefly, POPC and sterol solutions in $CHCl_3$ were mixed in the indicated proportions, dried under a gentle stream of nitrogen to produce a thin lipid film, and further dried under reduced pressure for 1 h. The films were hydrated in hot (~80 °C, above the T_m of ESPM) phosphate-buffered saline (PBS; 10 mM Na_2HPO_4, 150 mM NaCl, 0.02 % NaN_3 (w/v), pH 7.0), vortexed vigorously for 60 s, vortexed again for 15 s in a water bath incubated at 80 °C for 5 min, and re-vortexed for 30 s. Suspensions were allowed to cool to room temperature (~22 °C) before the experiments were carried out.

To test ESPM-sterol mixtures for detergent sensitivity, the OD of 1 ml of MLVs (500 nmol total lipid) was read at 600 nm using an OOIBase32 (Dunedin, FL) UV-vis spectrophotometer before and after the addition of 40 µl of a 10 % (w/v) Triton X-100 solution and 60 min of incubation. The final detergent-lipid molar ratio was ~14:1. To quantitate the degree of detergent resistance, the percent OD remaining after treatment with Triton X-100 was calculated according to Eq. 1 (*67*):

$$\%\ OD_{600}\ \text{remaining} = OD_{600}\ (+\ \text{detergent}) / OD_{600}\ (-\text{detergent}) \times 100 \qquad \text{Eq 1}$$

As described in Chapter 1, monolayer experiments were conducted using a computer-controlled Kibron μ Trough S surface balance (Helsinki, Finland). Lipids films were spread from stock solutions of mixtures of pre-weighed dry lipids dissolved in HPLC-grade hexane-2-propanol (3:2) at appropriate proportions. The subphase for all compressions was pure water (purified through a Milli-Q (Millipore Corp., Bedford, MA) to a resistivity of 18 MΩ·cm. Binary films were spread using a digital 10 μl Hamilton syringe. Compressions, at a rate of ~4 $Å^2$/molecule/min, began after a 5-min delay to allow evaporation of the solvents.

Film data were collected using Filmware, a software package provided by Kibron, and the results were analyzed with Filmfit software (Creative Tensions, Austin, MN). Ideal additivity of binary lipid films is described by Eq. 2:

$$A_\pi = X_1(A_1)_\pi + (1 - X_1)\,(A_2)_\pi \qquad \text{Eq 2}$$

where X_1 and $(1- X_1)$ are mol fractions of component 1 and 2, and $(A_1)_\pi$ and $(A_2)_\pi$ are molecular areas of components 1 and 2 at surface pressure, π (*38*). Deviations from the linear relationship described by Eq. 2 imply non-ideal behavior, with negative deviations suggesting condensation of the films caused by molecular packing among the system components.

Results

All of the sterol tested supported the formation of Triton-resistant domains (Figure 2). However, an examination of the results reveals a significant difference in

the amount of sterol required to mediate the onset of domain formation. MLVs consisting of 20 mol% of 24-ketocholesterol or 6-ketocholesterol were more insoluble than MLVs containing cholesterol, but 24-ketocholesterol and 6-ketocholesterol both formed MLVs that were more soluble than cholesterol. At this composition, 25-ketocholesterol supported domain formation to the same extent as non-oxidized cholesterol. Increasing the mol fraction of sterol produced MLVs that were increasingly insensitive to detergent treatment, and MLVs consisting of ≥40 mol% sterol were insoluble under the conditions employed and to a similar extent regardless of the sterol structure. The exception is 25-ketocholesterol, which supported domain formation but to a lesser degree at high sterol mol fraction.

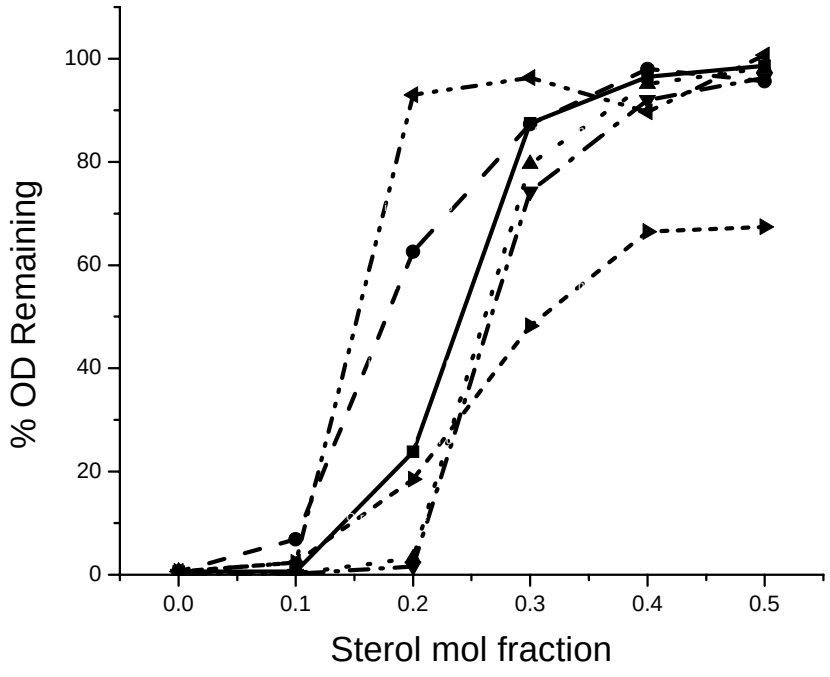

Figure 2. Plot of OD (600 nm) remaining after treatment of sterol-ESPM MLVs with Triton X-100. Cholesterol, ■, solid line; 6-ketocholesterol, ●, dashed line; 7-keto-

cholesterol, ▲, dotted line; 19-hydroxycholesterol, ▼, dash-dotted line; 24-keto-cholesterol, ◄, dashed-dotted-dotted line; 25-ketocholesterol, ►, short dashed line.

To qualitatively investigate the interactions of oxidized sterols with a different membrane lipid, the mean molecular area of sterol-POPC monomolecular films compressed at the air-water interface was plotted as a function of film composition. Figure 3 illustrates the differences in the condensation of POPC in the presence of oxygenated sterols. All of the sterols either mixed ideally or condensed POPC when present at a mol fraction of 0.1. However, differences began to emerge when the ratio of sterol:POPC was increased to 1:1 (Figure 4), and were dependent on the location of the oxygen atom within the sterol molecule. At this composition, only 6-ketocholesterol and 25-ketocholesterol behaved similarly to cholesterol. The effect of 6-ketocholesterol on the molecular area of POPC decreased at higher mol fraction of sterol, and that of 25-ketocholesterol was completely abolished, although mixing between sterol and POPC was ideal. Pronounced effects are seen for 7-ketocholesterol and 24-ketocholesterol (Figure 3, top panel; Figure 4, open bars), but are abolished at very high (90%) sterol mol fraction.

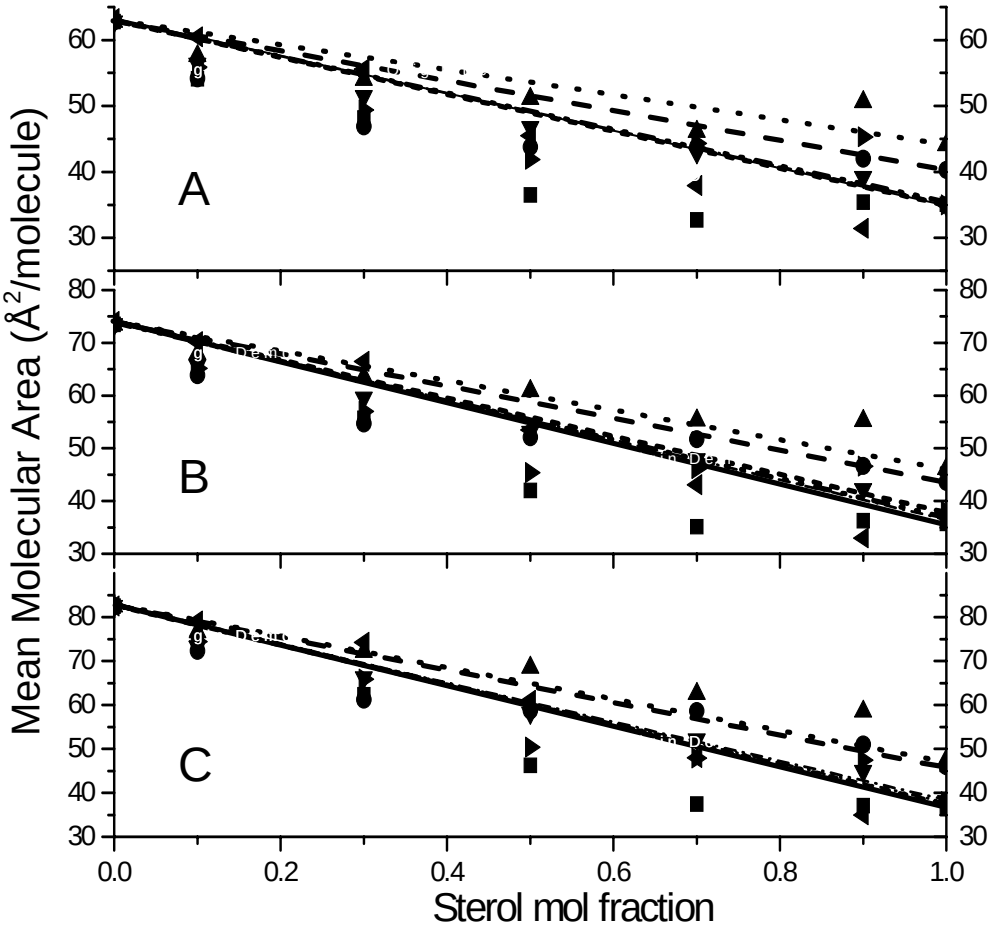

Figure 3. Area-composition curves for sterol-POPC monolayers at 20, 10, and 5 mN/m (A-C, respectively). Solid lines represent area if additivity were ideal. Cholesterol, ■, solid line; 6-ketocholesterol, ●, dashed line; 7-ketocholesterol, ▲, dotted line; 19-hydroxycholesterol, ▼, dash-dotted line; 24-ketocholesterol, ◄, dashed-dotted-dotted line; 25-ketocholesterol, ►, short dashed line.

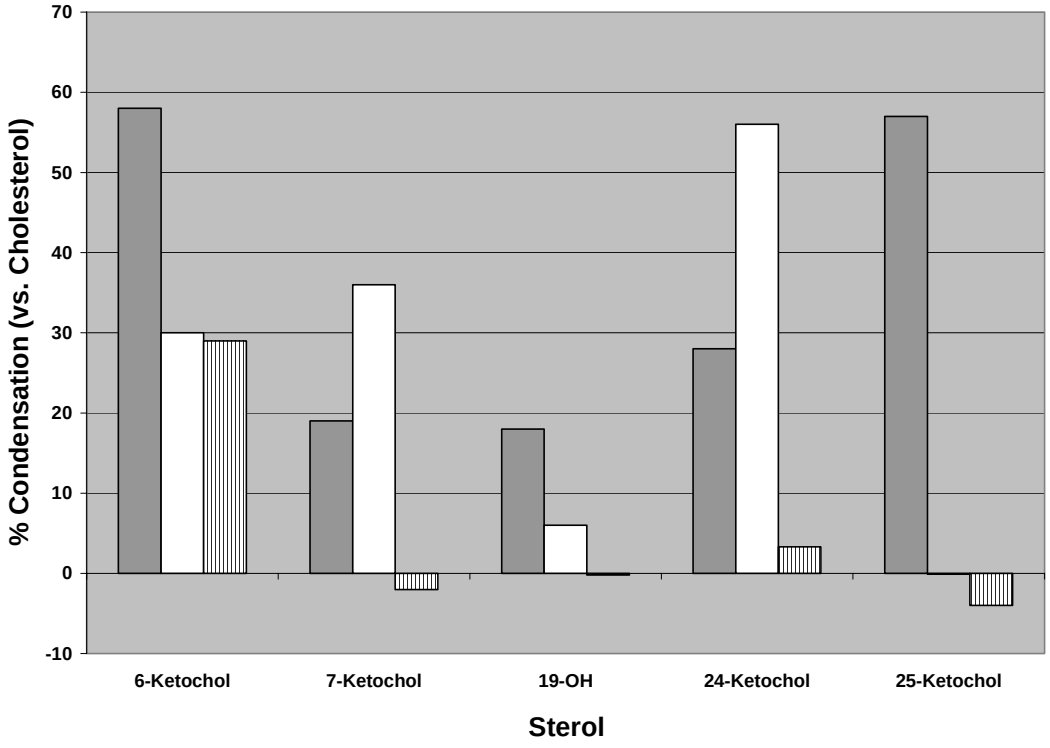

Figure 4. Condensation of POPC monolayers by oxygenated sterols as a percentage of condensation effect of cholesterol at 20 mN/m. Solid bars, 50 mol% sterol; open bars, 70 mol% sterol; hashed bars, 90 mol% sterol.

Discussion

The toxic effect of oxidized sterols on cells is well documented (*101, 102*), and several different sterol products of oxidative stress are known to exist in low-density lipoproteins (*67*). This study was designed to examine the extent to which these sterols differ in their interactions with ESPM and POPC in model membranes.

It has been reported that there is a correlation between the propensity of a sterol to support formation of insoluble lipid domains and its ability to condense phospholipid monolayers (*61, 67*). Both phenomena require the presence of liquid-

ordered (L_o) domains (*103*). Since insoluble lipid domains are important for some of the functions of membrane proteins, it follows that the local concentration of sterol needed to form these domains may have implications for the cell. It is, therefore, of interest to determine whether the presence of oxygenated sterols prevents their formation. The results described here indicate that some of the oxysterols studied perturb formation of DRMs, but others, at various mol fractions, actually enhance their formation.

The location of the oxygen atom in the sterol molecule has an effect on the interactions between the sterol and phospholipids, according to the results obtained in this study. A ketone group in close proximity to the 3β-hydroxy group (e.g., 6- and 7-ketocholesterol) alters the sterol's orientation with respect to the air-water interface (*63*); this is confirmed by the finding of a larger molecular area occupied compared to cholesterol (see the right-hand axis of Figure 3). The presence of the additional polar oxygen atom causes a tilt in the molecule, resulting in the observed increase in area. Moving the ketone farther away from the 3-hydroxy group changes the interactions with neighboring POPC or ESPM molecules, as can be seen by comparing results from the experiments with 6-ketocholesterol with 7-ketocholesterol in Figures 2, 3, and 4 (*104*).[2] It appears that an oxygen atom located at C7 interferes with intermolecular packing, preventing the tight interactions required for formation of the L_o phase. It is not known whether this is a result of steric hindrance or repulsion between oxygen in the sterol and the amide or ester chain in ESPM or POPC,

[2] It should be noted that 6-ketocholesterol lacks the C5,C6 double bond present in cholesterol and 7-ketocholesterol. However, cholestanol, a sterol differing from cholesterol only by the absence of the double bond, behaves similarly to cholesterol in model membranes. See Reference (27).

respectively, but this interference may help explain the toxic effects of 7-ketocholesterol in cells.

The position of the oxygen atom on the sterol side chain also affects the formation of L_o domains. The higher degree of DRM formation by 20 mol% 24-ketocholesterol compared to 25-ketocholesterol (and cholesterol) suggests that the onset of the L_o domain formation is disturbed by an oxygen atom near the end of the side chain. Evidently, the freer degree of mobility of a methyl ketone (25-ketocholesterol) compared to 24-ketocholesterol, in which the ketone is group is closer to the sterol ring system, affects interactions with neighboring lipids. The ideal mixing behavior of 19-hydroxycholesterol (Figure 3) and the results of the detergent solubility assay suggest that a hydroxy group at C19 interferes slightly with sterol-ESPM and sterol–POPC interactions compared to cholesterol, since 30 mol% sterol is required before detergent insoluble domains are formed (Figure 2). The difference in the behavior of 19-hydroxycholesterol and the keto-containing sterols may result from the presence of a hydrogen bond donor not present in the keto sterols. It is of interest to note, however, that a toxic sterol, like 7-ketocholesterol, differs from native cholesterol with respect to the relative amount present before the L_o phase forms. For 7-ketocholesterol, 20 mol% sterol forms highly insoluble membranes, and, at the same sterol:ESPM molar ratio, 19-hydroxycholesterol/ESPM membranes are dissolved essentially completely by Triton. Thus, the local concentration of sterol appears to be important for DRM formation and concomitant function of proteins and processes that may be associated with it.

Summary

An investigation into the behavior of 6-, 7-, 24-, and 25-ketocholesterol and 19-hydroxycholesterol in model membranes reveals that the presence of an extra oxygen atom causes significant differences in lipid-lipid interactions. Placement of the oxygen atom one carbon farther away from the 3β-hydroxy group of cholesterol affects sterol-ESPM and sterol-POPC interactions as determined by detergent solubility and monolayer assays. The study also illustrates the sensitivity of cholesterol's behavior in model membranes to the presence and location of oxygen in the side chain, where it was found that, depending on the mol fraction of sterol in the bilayer, moving the carbonyl group from C24 to C25 causes changes in the way the sterol interacts with both ESPM and POPC.

Chapter 5

Lysophosphatidic Acid and Lipopolysaccharide Bind to the PIP_2-Binding Domain of the Actin-Severing Protein Gelsolin

Abstract

The actin-severing protein gelsolin is regulated mainly by phosphatidylinositol 4,5-bisphosphate (PIP_2). We report here ITC studies on the interactions of the P2 peptide (residues 150-169) with lysophosphatidic acid (LPA) and lipopolysaccharide (LPS). The binding to 1-oleoyl-LPA is exothermic at both 25 °C and 37 °C, and K_d increased from 0.92 μM to 24 μM on addition of 150 mM NaCl at 25 °C, indicative of the role of ionic interactions in P2 binding to LPA. The ΔH° was -2.07 kcal/mol in the absence of salt and -0.23 kcal/mol in the presence of 150 mM NaCl at 25 °C. The interaction of lipopolysaccharide (LPS) from *P. aeruginosa* with gelsolin P2 was stronger than that of LPA with P2; at pH 7.4 and in the absence of salt, K_d was 177 nM, and ΔH° was -7.6 kcal/mol at 25 °C.

Introduction

Lysophosphatidic acid (LPA) is structurally the simplest of the glycerophospholipids (Figure 1). LPA is produced in various types of cells via *de novo* synthesis from the early lipid metabolic intermediate glycerol-3-phosphate or by deacylation of phosphatidic acid and is secreted by activated platelets and other cells (*105-107*). This phospholipid growth factor displays a myriad of cellular functions,

the best understood of which are mediated through high affinity binding to the products of several members of the EDG (Endothelial Differentiation Genes) family of G-protein-coupled receptors (GPCR) genes (*108*). Examples of activities that are controlled by the interactions of LPA with GPCR (*108, 109*) are smooth muscle contraction, Ca^{2+} efflux, and neurotransmitter regulation. LPA also regulates the actin-binding and actin-severing activities of gelsolin (*110, 111*).

Recent research has revealed that LPS (Figure 2), a complex, high-molecular weight negatively charged lipid that in large part forms the outer membrane of Gram-negative bacteria, also binds to gelsolin (*112*). In place of the glycerol backbone present in LPA, LPS has an acylated glucosamine backbone. LPS consists of lipid A, which is typically a disaccharide of glucosamine derivatized as a mono-or diphosphate, and as many as seven fatty acyl chains *(113, 114)*. The lipid A component of LPS is responsible for the toxic properties of the LPS molecule (*114*). Lipid A is glycosylated in many bacteria with two 3-deoxy-D-manno-octulosonic acid residues (termed KDO), and an oligosaccharide that comprises the carbohydrate backbone (*115*). The variable size and non-repeating sequences of the sugar sequence are responsible for recognition of antigens to various strains of endotoxin (*116*).

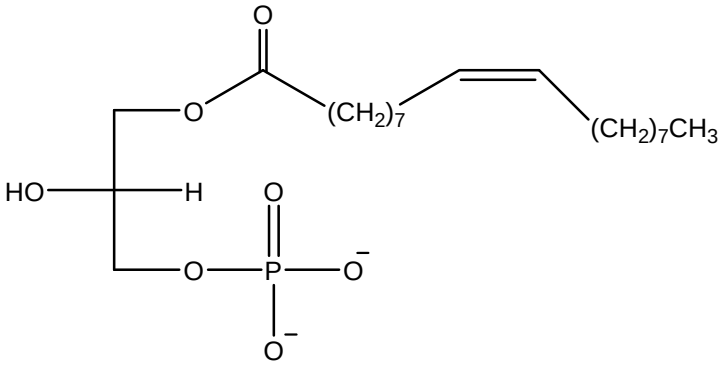

Figure 1. 1-Oleoyl-LPA

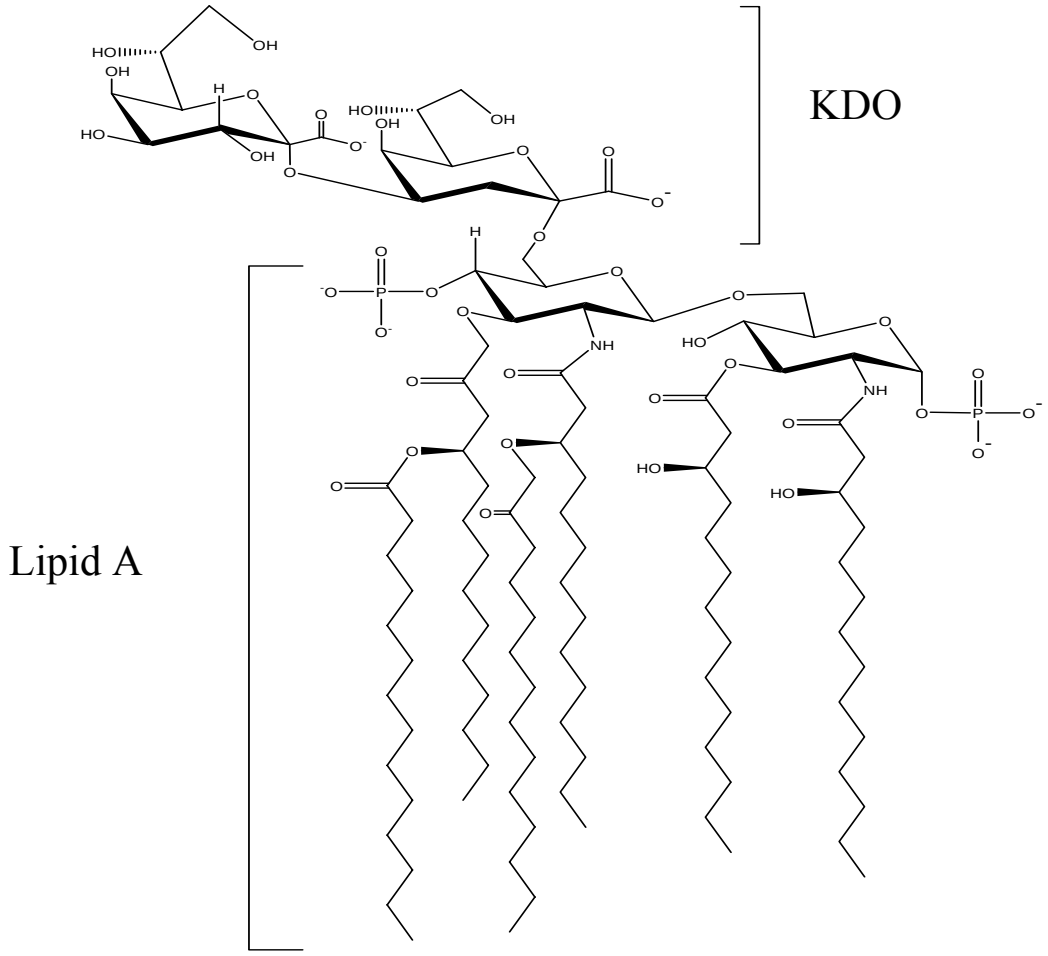

Figure 2. General structural features of lipopolysaccharide

Gelsolin is an approximately 85-kDa protein present in plasma and in extracellular fluids at concentrations of 100-250 μg/ml (*117*). This protein regulates cellular morphology and motility by severing actin filaments, binding actin monomers, and nucleating actin polymerization, resulting in cytoskeletal modifications (*110, 118*). It is mainly regulated by phosphatidylinositol 4,5-bisphosphate (PIP_2) (*119, 120*) through binding at two sites near the *N*-terminus of the protein (*110, 121*), denoted as P1 (residues 135-149) and P2 (residues 150-169, Figure 3). P2 was shown to compete with full-length gelsolin for binding to PIP_2 (*121*).

KHVVPNEVVVQRLFQVKGRR-OH

Figure 3. Gelsolin sequence 150-169, denoted as P2.

The discovery that LPA was as efficient as PIP_2 in dissociating related actin-binding protein complexes (*122*) suggests an additional role for this lipid, i.e., as a regulator of cellular structural reorganization via interactions with gelsolin.

Sepsis is a major cause of human deaths. It is triggered when LPS is released from the outer cell wall of Gram-negative bacteria (*123*). LPS binds to a plasma protein known as LPS-binding protein (LBP), and subsequently undergoes trafficking to cell membranes with the CD14 receptor and to Toll-like receptors (*124-126*). The interaction of LPS with plasma proteins is of great interest, since there is an obvious potential therapeutic utility if such a complex leads to inactivation of the cytotoxic effects of LPS.

In the work presented in this chapter, the thermodynamics of LPA and LPS interactions with the P2 domain of gelsolin have been characterized and compared by ITC.

Materials and Methods

Gelsolin P1 was kindly supplied by Prof. Paul Janmey at the University of Pennsylvania. Gelsolin P2 was generously provided by Prof. Fred Naider and Dr. Hasmik Sargsyan at the College of Staten Island, CUNY. 1-Oleoyl-LPA, 1-myristoyl-LPA, and 1-palmitoyl-lysophosphatidylcholine (LPC) were purchased from Avanti Polar Lipids (Alabaster, AL) and were used without further purification. LPS from *P. aeruginosa* was purchased as the lyophilized powder from Sigma-Aldrich (St. Louis, MO).

LPA was dissolved in buffer consisting of 10 mM HEPES, 0.1 mM EDTA, pH 7.4, with or without NaCl, to a concentration of ~5 mM (see figure captions for concentrations) and vortexed vigorously for ~2 min at room temperature. Mixtures of LPC and LPA were prepared by dissolving LPC and LPA in $CHCl_3$, followed by evaporation under a stream of N_2 until a thin lipid film remained. The film was dried further under vacuum overnight and hydrated with buffer, vortexed vigorously for ~5 min, and sonicated in a water bath at room temperature. Gelsolin P1 and P2 were dissolved in 10 mM HEPES buffer, pH 7.4, at concentrations of 74-136 μM, and the solution was vortexed gently for 1 min and sonicated in a water bath at room temperature for 5 min. Buffers were prepared with ultra-pure water (distilled and

passed through a Milli-Q water purification system (Millipore Crop., Bedford, MA) to a resistivity of 18 MΩ cm).

High-sensitivity ITC was conducted in a Microcal MCS calorimeter (Northampton, MA) at 25 and 37 °C. All solutions were degassed with stirring for at least 30 min prior to experiments. The 250-µl injection syringe was loaded with LPA solution and 8-10 µl aliquots were injected into the ITC sample cell containing P2, after temperature equilibration, at 4-min intervals. The contents of the sample cell were stirred at a rate of 400 rpm throughout the experiment.

For the LPS-binding experiments, the titration was carried out by filling the syringe with P2 and the sample cell with LPS. P2 and LPS were dissolved in 10 mM dibasic sodium phosphate, pH 7.4 (in the absence of NaCl). Aliquots of 6 µl of 136 µM P2 were injected into 2.7 µM LPS at 4-min intervals and stirred as described above.

Data were collected and analyzed using Origin 5.0, a software package provided by Microcal. Best-curve fit routines by Origin of the integrated area under the peaks of the raw data were performed using a one-binding-site model, from which the values of $\Delta H°$ and $\Delta S°$ were obtained. The dissociation constant K_d and Gibbs free energy change were obtained from the fundamental equations of thermodynamics, $\Delta G° = -RT \ln K = \Delta H° - T\Delta S°$.

Results

LPA-P2 Interactions

Figure 4a shows the results of a titration of 74 μM P2 with 4.9 mM LPA at 25 °C in the absence of salt. To determine the contributions of ionic interactions, the binding was studied with increasing concentrations of NaCl (Figure 4b,c). The interactions in all of the titrations are exothermic, and the results are summarized in Table 1. Increasing the salt concentration caused the reaction to become less exothermic, from -2.1 kcal/mol in the absence of salt to -0.23 kcal/mol in the presence of 150 mM NaCl. The K_d decreased with lower salt concentration, from 24 μM in the presence of 150 mM NaCl to 0.92 μM in the absence of salt.

Table 1. Thermodynamic data for the interaction of 1-oleoyl-LPA with gelsolin P2 at 25 °C. Errors from 2-3 trials were within a standard deviation of ± 15%.

[NaCl] (mM)	ΔH° (kcal/mol)	TΔS° (kcal/mol)	ΔG° (kcal/mol)	K_d (μM)
0	-2.1	6.1	-8.2	0.92
100	-0.96	5.9	-6.9	9.0
150	-0.23	6.1	-5.8	24

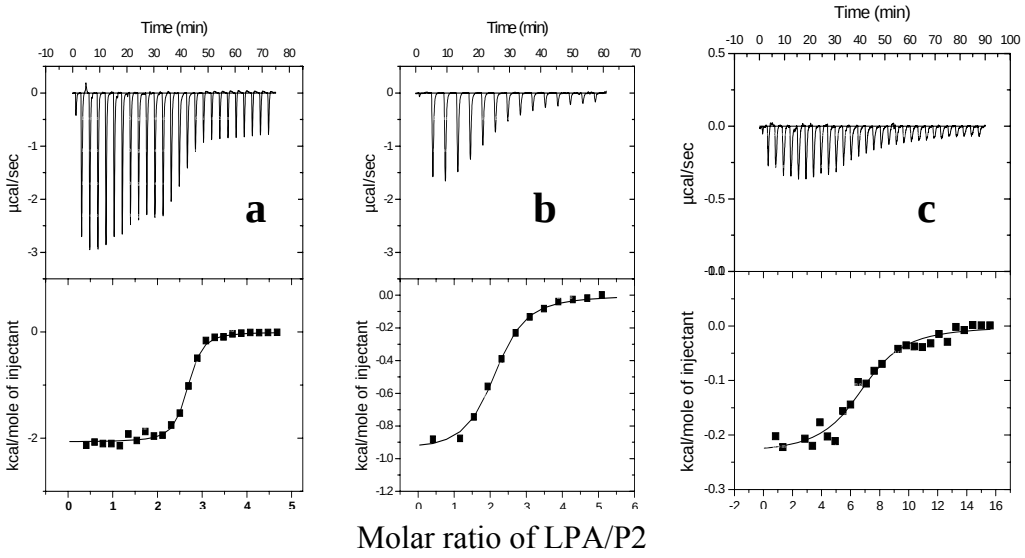

Figure 4. Upper panels: ITC traces of binding of 74 µM gelsolin P2 with 4.9 mM 1-oleoyl-LPA in (*a*) the absence of NaCl, and in the presence of (*b*) 100 mM NaCl, and (*c*) 150 mM NaCl at 25 °C. Lower panels: Integrated data from top showing best fit curves. See Materials and Methods for experimental details.

The structural specificity with respect to the acyl chain of LPA and P2 was examined by titrating P2 with 1-myristoyl-LPA. As shown in Figure 5, an exothermic heat of binding was detected but did not reach saturation, indicating non-specific interactions. Ionic interactions appear to be important since no discernible binding (i.e., no heat change detected; data not shown) was observed when the buffer contained 150 mM NaCl.

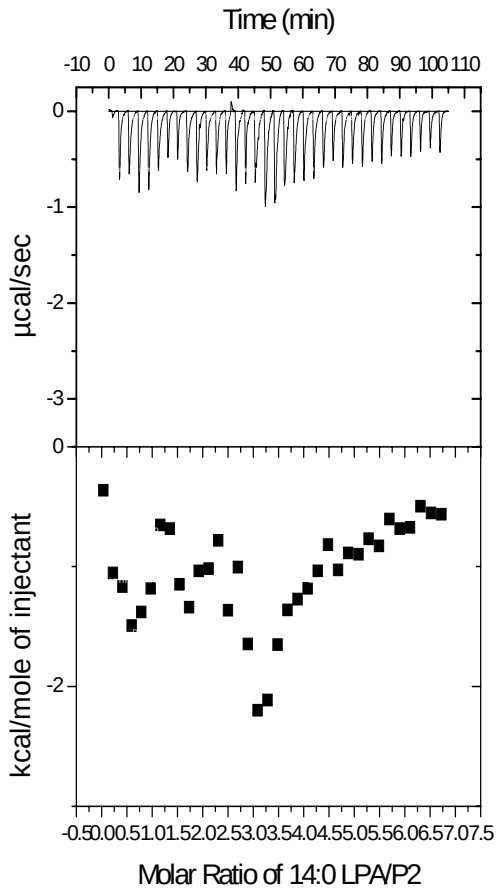

Figure 5. Titration isotherm of binding of 100 µM P2 with 5 mM 1-myristoyl-LPA in buffer without NaCl at 25 °C.

When P2 was titrated with 1-palmitoyl-LPC no binding was detected in buffer containing 100 mM NaCl. (Figure 6, top panel, curve a). As summarized in Table 2, when the LPA/LPC ratio was increased from 1:1 to 1.6:1 (mol/mol), ΔS° was unchanged and ΔH° became slightly more negative (Figure 6, curve c, and Table 2), and the binding affinity increased slightly (K_d decreased from 40 µM to 27 µM). To confirm that the heat signal detected was a result of binding of LPA to P2 and not to demicellization of the LPA/LPC aggregate, the same solution of LPA/LPC was

injected into the buffer, and an insignificant heat change was observed (Figure 6, top panel, curve b).

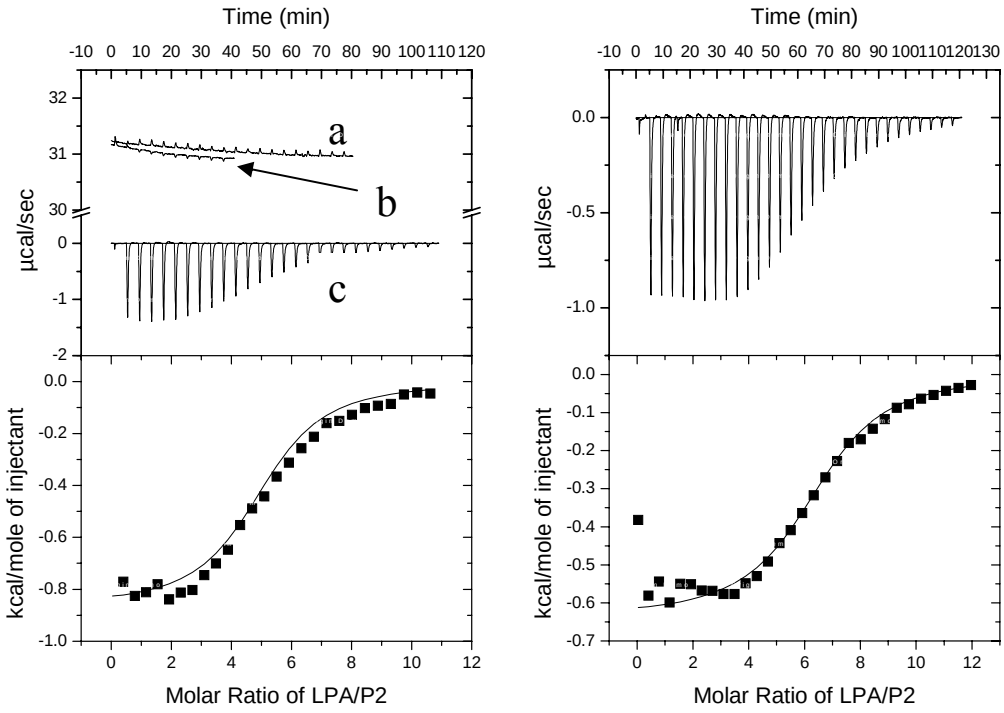

Figure 6. Binding isotherms of 1-oleoyl-LPA/1-palmitoyl-LPC mixtures with P2. Top panels represent raw ITC data; bottom panels represent integrated heats/mol injectant. Curve a, LPC injected into a solution of P2; curve b, LPA/LPC mixture injected into a solution of pure buffer; curve c, LPA/LPC mixture (left panel, 1.6/1; right panel, 1/1 (mol/mol)) injected into P2. Titrations were performed at 25 °C in buffer containing 100 mM NaCl. The concentration of 1-oleoyl-LPA in the syringe was 5 mM; the P2 concentration was 100 µM.

Table 2. Thermodynamic data for the interaction of 1-oleoyl-LPA/1-palmitoyl-LPC mixed micelles with gelsolin P2 in 100 mM NaCl at 25 °C. Errors from 2-3 trials were within a standard deviation of ± 5%.

LPA/LPC (mol/mol)	K_d (μM)	ΔH° (kcal/mol)	TΔS° (kcal/mol)
1:1	40	-0.64	5.4
1.6:1	27	-0.87	5.4

The effect of temperature on the binding of LPA to P2 was determined by performing ITC studies at 37 °C and 150 mM NaCl. The interaction was more exothermic at the higher temperature, and K_d decreased (Table 3). The difference in ΔH° observed at the two temperatures allows the calculation of the change in heat capacity (ΔC_p) according to the Kirchoff equation, Eq. 1 (*127-129*):

$$\Delta C_p = d(\Delta H^\circ)/d(T) \qquad \text{Eq. 1}$$

The value for ΔC_p calculated from Eq. 1 was -29.5 cal/K. A negative value for ΔC_p suggests hydrophobic dehydration on binding (*127, 130*).

Table 3. Thermodynamic data for 1-oleoyl-LPA/gelsolin P2 interactions in 150 mM NaCl HEPES buffer (pH 7.4) at 25 °C and 37 °C. Errors from 2-3 trials were within a standard deviation of ± 20%.

Temperature (K)	ΔH° (kcal/mol)	K_d (μM)
298	-0.23	24
310	-0.59	14

LPS-P2 Interactions

To study the binding of LPS to P2, the sample cell was filled with 2.7 μM LPS and titrated with 136 μM P2 in salt-free 10 mM sodium phosphate buffer, pH 7.4 at 25 °C. The results are shown in Figure 7. The data reveal that P2 binds with a higher affinity to LPS (K_d = 177 nM) than to 1-oleoyl-LPA (K_d = 0.92 μM) under the same experimental conditions, and that the binding is considerably more exothermic (ΔH° = -7.6 kcal/mol), although the lipids were suspended in different buffers. These results are consistent with recent work showing strong interactions between LPS and a rhodamine-labeled 10-residue peptide (gelsolin residues 160-169) derived from P2 (*112*). The binding was considered to be highly specific because no interactions were detected when P2 was replaced with a peptide in which the sequence of amino acids was scrambled.

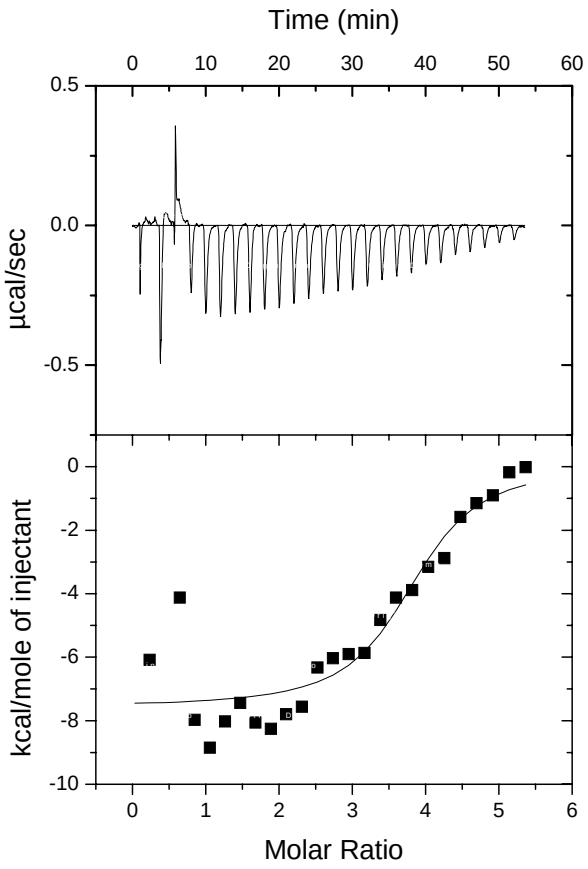

Figure 7. Titration isotherm of binding of LPS with P2 in sodium phosphate buffer, pH 7.4, at 25 ºC.

Discussion

LPA-P2 Interactions

It has been shown previously that LPA binds to full-length, plasma gelsolin (*117, 122*), and very recently the binding of gelsolin to LPS from *Salmonella minnesota* was also demonstrated (*8*). The goal of the studies described in this chapter was to investigate in more detail the thermodynamics of the interactions of

LPA and LPS with one of the two known peptides that comprise part of gelsolin's binding site for polyphosphoinositides.

The equilibrium binding of LPA with P2 is sensitive to the presence of NaCl in the buffer system (Table 1). The peptide bears 5 positive charges and LPA bears ~1.5 negative charges at the experimental pH; therefore, the finding of an electrostatic component of the binding is not surprising. The addition of salt to the buffer shields the charged groups on P2 and LPA, decreasing affinity. However, although K_d and $\Delta H°$ both become more favorable as the salt concentration is decreased, binding is not abolished even in 150 mM NaCl, and K_d is still in the low micromolar range. The stoichiometry may be expected to reflect complete charge compensation between the peptide and a negatively charged lipid if the binding arises exclusively via electrostatics (*127*). Additional evidence for the existence of specificity for LPA-P2 binding is provided by the facts that no interactions were detected between LPA and the second PIP_2-binding domain, P1 (data not shown), and that PIP_2 binds with high affinity to an engineered P2 analog bearing a net negative charge (*118*). The fact that replacing 1-oleoyl-LPA with 1-myristoyl-LPA resulted in an exothermic but unsaturable isotherm also suggests that charge attraction is insufficient to fully account for the high affinity binding (Figure 4).

Intestinal fatty acid binding protein interacts with lipids via electrostatics to create a "collisional complex," after which hydrophobic forces appear to drive the high affinity binding (*131*). It is likely that a similar phenomenon occurs with P2, with the ionic forces between P2 and LPA bringing the species into close proximity prior to hydrophobic binding.

LPA/LPC Interactions with P2

LPC, which is structurally similar to LPA, also appears to interact with various GPCRs (*132*). The lipids differ in their head group structure, which is apparently sufficient to prevent LPC from binding to P2. The absence of a net negative charge in LPC may prevent the formation of the collisional complex that appears to be required for binding with P2. LPA retains its ability to bind with high affinity to P2 in mixed micelles with LPC, suggesting that the affinity of the LPA-P2 interaction is sufficient to overcome the forces between LPA and LPC in the micelle.

LPS-P2 Interactions

The negative heat capacity obtained from these studies[3] suggests that hydrophobic dehydration of the charges occurs on binding of LPA to P2 (*127, 128*). This has been observed for the binding of LPS with the polycationic drug polymyxin B (*127*). That P2 interacts with LPS is not surprising since the polycationic character of P2 is one of the structural requirements found to be important for LPS-binding properties, the others being cationic protonatable groups residing approximately 15 Å apart and a hydrophobic moiety (*123*). The high affinity of P2 for LPS suggested by K_d in the nanomolar range (Figure 7), and the results of Bucki et al. showing a high degree of specificity of the peptide for LPS (*8*), suggest a role for gelsolin in the transport of the toxin through the bloodstream. Gelsolin levels decrease during trauma, and low levels of the protein coincide with greater susceptibility to shock

[3] A rigorous application of the Kirchoff relationship requires additional experiments at other temperatures.

(*133*). Thus, LPS appears to be another lipid, in addition to polyphosphoinositides and LPA, that can interact with and affect the levels of gelsolin in plasma.

Additional ITC experiments, including the investigation of the effects of temperature, divalent cations, and pH, may provide a more complete understanding of the mechanism of the P2-LPA and P2-LPS interactions. Circular dichroism spectroscopy may be used to determine the extent of secondary structural alterations that the peptide may undergo as a result of its interactions with LPA and LPS.

Summary

ITC was employed to study the interactions of the PIP_2-binding domain of gelsolin with LPA and LPS. Gelsolin P2 did not bind to LPC, and LPC did not interfere with LPA binding with P2. The binding of P2 to LPS from *P. aeruginosa* was tighter than to 1-oleoyl-LPA and 1-myristoyl-LPA. These results quantify very recent data showing strong and selective binding of a shorter peptide derived from P2 to LPS (*112*). Equilibrium constants for P2-LPA interactions were in the micromolar range, and $\Delta H°$ and $\Delta S°$ were both thermodynamically favorable and salt- and temperature-dependent, but binding remained strong whether or not NaCl was present at both temperatures used in the study.

Chapter 6

The Critical Micelle Concentration of Lysophosphatidic Acid and Sphingosylphosphorylcholine

Abstract

The critical micelle concentrations (CMCs) of lysophosphatidic acid of various acyl chain lengths and in solutions containing different amounts of NaCl were measured by ITC. A strong salt dependence was observed, with CMCs decreasing in a non-linear trend, from 0.188 mM in the absence of salt to 0.060 mM in 150 mM NaCl. The CMC was also sensitive to the number of methylene groups in the acyl chain. No such salt dependence was observed for the CMC of sphingosylphosphorylcholine (SPC). Reduction of the double bond of SPC to form 4,5-dihydro-SPC lowered the CMC value from 0.158 mM to 0.056 mM in phosphate buffer, pH 7.4.

Introduction

Lysophosphatidic acid (1-acyl-2-lyso-*sn*-glycero-3-phosphatidic acid, LPA, Figure 1a) is the structurally simplest glycerophospholipid. Studies of its cellular activities have been conducted over a range of lysolipid concentrations. LPA produces its effects, including calcium efflux, platelet aggregation, cell growth and death (apoptosis), and neurotransmitter release, through its interactions with G protein-coupled receptors (GPCR) of the Endothelial Differentiation Gene (EDG) family (*107-109*) as well as through other, non-GPCR membrane proteins (*134*).

Sphingosylphosphorylcholine (SPC, Figure 1b) is another lysophospholipid that is structurally similar to LPA, but has a sphingosine backbone instead of a glycerol backbone, and also exerts cell signaling activities (*135*), but its specific membrane receptors have not yet been identified with certainty (*136*).

The structures of LPA and SPC are conducive to the formation of micelles, and it is therefore of interest to determine the aggregation state that these amphiphiles adopt under physiological conditions. Specifically, it is not clear whether LPA in circulation exists as monomers or as micelles. The study described in this chapter applies ITC to measure the critical micelle concentration (CMC) of LPA, SPC, and dihydro-SPC, in which the C4,C5 double bond of SPC is reduced (Figure 1c), and to determine the effect of salt concentration on the CMC values. The effect of acyl chain length of LPA on the CMC is also presented here.

The use of ITC for CMC determination offers several advantages over other methods. The technique's reliance on heat changes that accompany the decomposition of the micelle negates the requirement for fluorescent or other spectroscopic probes, which can perturb the measurements (*137, 138*). Additionally, the thermodynamic parameters of the process can be obtained from one experiment. Finally, the material is easily recycled as no exogenous reagents are used.

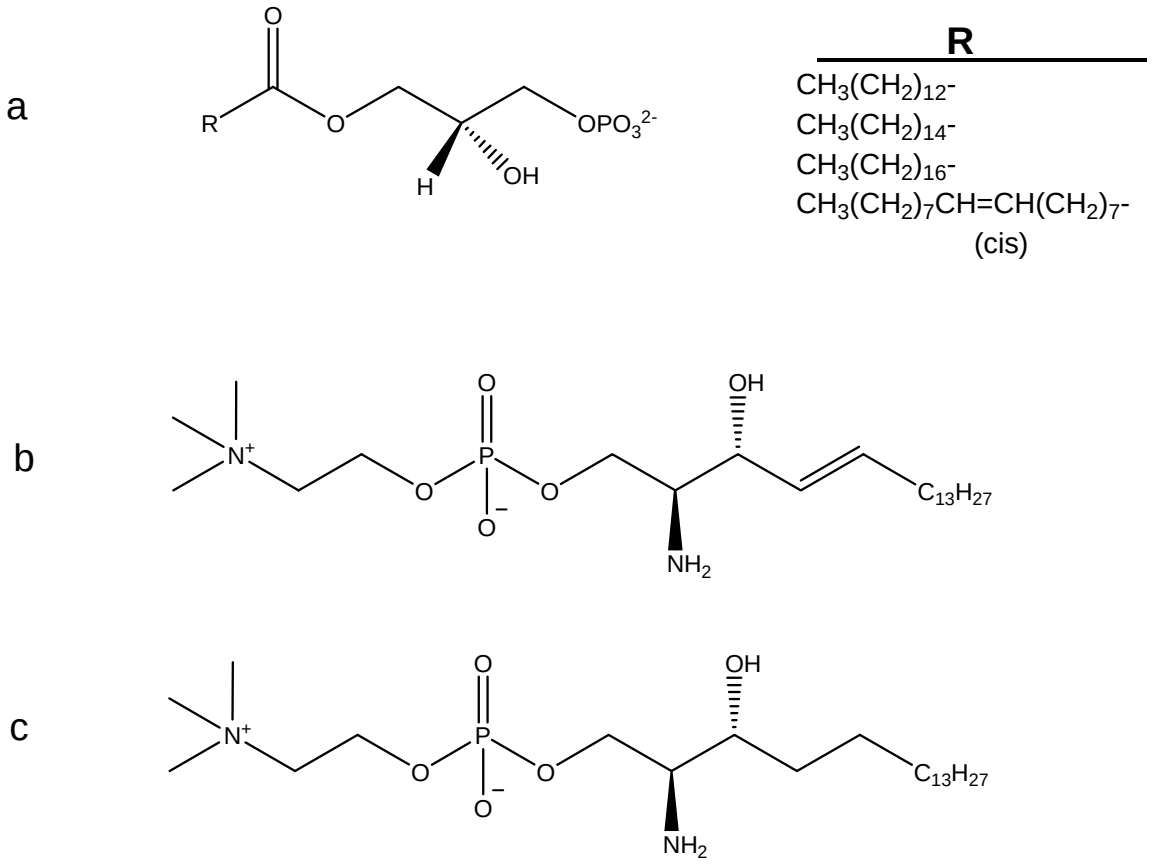

Figure 1. a, LPA; b, SPC; c, 4,5-dihydro-SPC.

Materials and Methods

LPA and SPC were purchased from Avanti Polar Lipids (Alabaster, AL). Dihydro-SPC was prepared by catalytic hydrogenation of SPC by Dr. Kucharani Jacob. Octyl β-thioglucoside and Triton X-100 were from Sigma-Aldrich (St. Louis, MO).

ITC was conducted using a Microcal MCS microcalorimeter (Northampton, MA) at 25°C. Lipids (or detergent) were weighed and dissolved in water or sodium phosphate buffer (pH 7.4) with or without NaCl and were vortexed vigorously until a

clear suspension resulted. All solutions were degassed with stirring for at least 15 min prior to experiments.

The method of measuring the CMCs of detergents using ITC has been described previously (*137*). Aliquots of a concentrated solution of the amphiphile are injected into the sample cell containing water or buffer, allowing equilibrium to be achieved between injections. The heat change from each dilution, resulting from the disassembly of the aggregate structure (demicellization) is plotted as a function of time. The inflection point of the curve resulting from integration of the raw data is taken as the CMC value (*128, 137, 139*).

Experimentally, a 250-µl syringe was loaded with lipid suspension at high concentration (>>CMC), and the sample and reference cells were filled with the same buffer (or water) used to dissolve the lipids. Each experiment was initiated by injecting a 1-µl aliquot into the sample cell after allowing equilibration of temperature. (The heat from this first injection was ignored in the data analysis.) Thereafter, 5-10 µl aliquots were injected at 4-min intervals. The contents of the cell were stirred by the computer-controlled syringe at a rate of 400 rpm. The sample cell was rinsed repeatedly with pure water and the syringe was cleaned with water and EtOH between experiments. Data were analyzed using Origin 5.0. Some of the ITC experiments were carried out by Dr. Zaiguo Li.

Results and Discussion

In order to confirm the suitability of ITC as a method to measure CMCs, we applied the technique to two detergents, Triton X-100 (Figure 2) and octyl β-

thioglucoside (data not shown), whose CMC values were reported previously. Our ITC results are consistent with those reported for both detergents (11.23 ± 0.02 mM at 25 °C vs. 15.94 mM at 60 °C for octyl β-thioglucoside (*139*) and 0.22 ± 0.01 mM for Triton X-100 at 25 °C vs. 0.20-0.90 mM).[4]

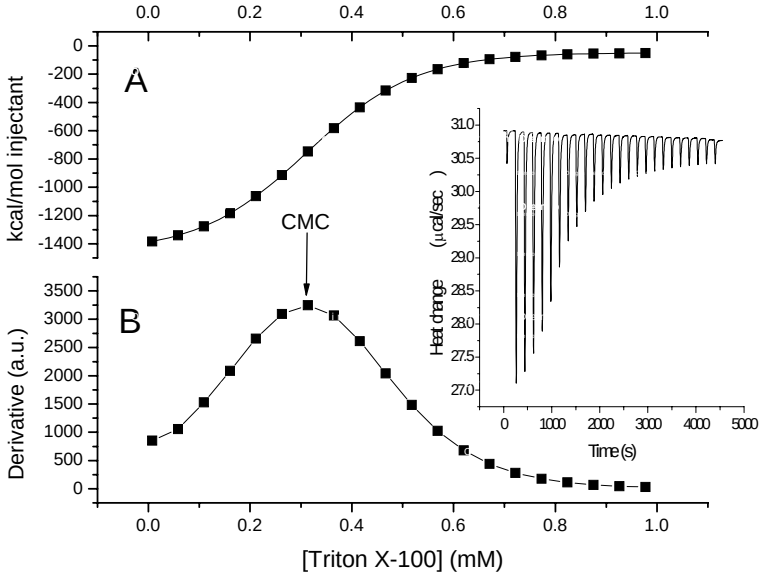

Figure 2. Isothermal titration of Triton X-100 into pure water. A, heat observed on injection of 10-μl aliquots of a Triton X-100 suspension in water (10 mM) into the sample cell (volume, 1.35 ml) at 25 °C. B, first derivative of curve in A. The CMC is the maximum of the derivative; inset, measured heat power vs. time elapsed during serial injections.

[4] (*Merck Index* **13**, 6793)

Figure 3 shows the results from a titration of 1-oleoyl-LPA into pure water. The raw data (inset) indicate that the demicellization for this lipid is endothermic. The CMC is 0.346 mM.

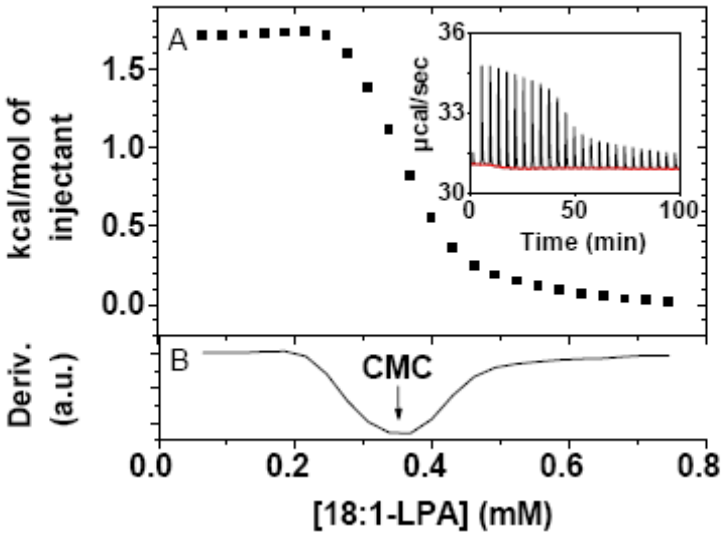

Figure 3. Results from ITC demicellization experiment of 1-oleoyl-LPA in pure water. A, heat absorbed per injection of 7.96 mM LPA vs. final LPA concentration in the 1.35 ml sample cell. B, first derivative of curve from A (the minimum is taken as the CMC); inset, raw ITC data showing heat vs. time. (From (*18*).)

To investigate the effect of increasing salt concentration on the CMC of 1-oleoyl-LPA and SPC, a series of experiments was performed using serially diluted solutions of NaCl in the solvent. The CMC of LPA displayed a strong dependence on salt concentration, decreasing exponentially with increasing NaCl concentration (Figure 4). A limiting CMC value of ~60 µM was reached at 160 mM NaCl. This result indicates that the phosphate groups of neighboring LPA molecules are shielded by sodium ions, decreasing repulsion within the micellar structure. No such salt

dependence was observed with SPC, perhaps because of its zwitterionic choline headgroup and protonatable 2-amino functionality.

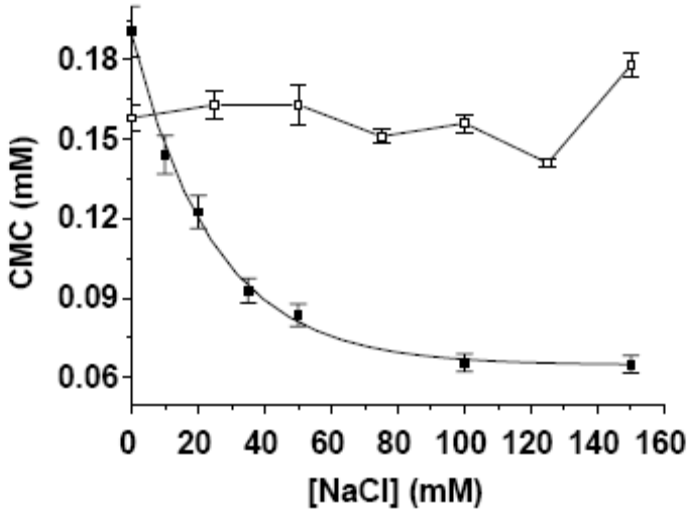

Figure 4. Dependence of CMC values of 1-oleoyl-LPA (solid squares) and SPC (open squares) on NaCl concentration at 25 °C. (From (*18*)).

Since increasing chain length affects the water-accessible region of hydrocarbon chains, the CMC is highly dependent on the number of methylene groups (*128*). Table 1 shows the CMC values of synthetic LPAs with increasing chain length in pure water at 25 °C. The kink introduced into the acyl chain of LPA by addition of one cis double bond increases the CMC by a factor of ~4, probably because of less efficient lipid packing in the micelles. This behavior was also observed when the double bond of SPC was reduced.

The CMC for SPC in 10 mM monobasic sodium phosphate, pH 7.4, at 25 °C is 0.158 mM (Figure 5), and removal of the double bond reduced the CMC by a factor of 3, to 0.056 mM.

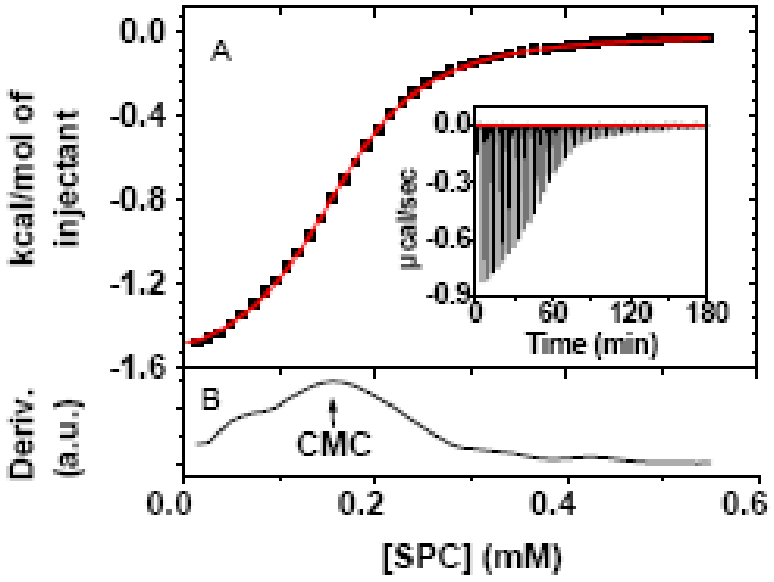

Figure 5. ITC demicellization of SPC in 10 mM sodium phosphate, pH 7.4, at 25 °C, in the absence of NaCl. A, Heat evolved as a function of $[SPC]_{Final,\ cell}$; B, first derivative of curve in A. The maximum is taken as the CMC; inset, heat signal per injection. (From (*18*).)

Table 1. Effect of acyl chain on CMC values of LPA in water at 25 °C. Errors were ± 10% from duplicate or triplicate titrations.

Acyl chain	CMC (mM)
14:0	1.850
16:0	0.540
18:0	0.082
18:1Δ^9 cis	0.346

The contribution of each methylene group to the ΔH° of micelle formation can be obtained by plotting the change in enthalpy as a function of methylene groups in the acyl chain (*128*). A value of -1.14 kcal/mol/methylene group was obtained, which is higher than that observed for lysophosphatidylcholine (LPC) by Heerklotz and

Epand (-0.478 kcal/mol (*128*)). Comparison of the CMCs of LPA and LPC of identical acyl chain lengths and structures obtained by ITC measurements demonstrate a much higher value for the former in pure water at the experimental temperature. Identical values of CMCs were obtained for LPCs whether the measurements were taken in pure water or in 150 mM buffer (pH 7.4) (*128*). This is in contrast to the results reported here for LPA, where a strong salt-dependence was observed (Figure 4), but similar to the results obtained with another phosphocholine-containing lysolipid, SPC.

Summary

ITC was employed to measure the CMC of LPAs consisting of various acyl chains as a function of NaCl concentration at 25 °C. A strong salt dependence was observed, and the CMC increased significantly when one cis double bond was introduced into the acyl chain. No salt dependence was observed for the CMC of SPC. Catalytic hydrogenation of the double bond of SPC to form 4,5-dihydro-SPC resulted in a decrease in the CMC value. Based on the low CMCs observed in the presence of NaCl, it is reasonable to hypothesize that LPA perform many of their biophysical actions as micellar aggragates.

Chapter 7

Implications For Future Research

The results described in this thesis indicate that some of the photoactivatable and fluorescent cholesterol analogs described herein can be considered to be useful sterol probes. Future studies of cholesterol transport, identification of proteins that bind to cholesterol, and additional features important for the formation of membrane domains can be proposed using these molecules.

The findings of the differing ability of oxysterols to support L_o domains presented in this thesis may be useful for future studies on the membrane behavior of oxysterols, and the extent to which lipid raft formation is at least partly responsible for the cytotoxicity of specific oxysterols.

The determination of the aggregation state of LPA under physiological conditions as reported in this thesis has significant implications in light of the involvement of this lysophospholipid in signaling, cell growth, and apoptosis. The information presented about gelsolin-LPA interactions, and the potential relationships between cytoskeletal changes and the presence of LPA (*140, 141*), contributes to the known data on this research subject. The data from the ITC experiments on LPS and gelsolin reported here provide quantitative support for the recent report of the interaction of gelsolin and LPS. The search for an agent to sequester LPS may have therapeutic potential; the finding that a short peptide derived from gelsolin binds with nanomolar affinity to LPS suggests a possible avenue of pursuit.

References

(1) Wenk, M. R. (2005) The emerging field of lipidomics. *Nat. Rev. Drug Discov. 4*, 594-610.

(2) Umezu-Goto, M., Tanyi, J., Lahad, J., Liu, S., Yu, S., Lapushin, R., Hasegawa, Y., Lu, Y., Trost, R., Bevers, T., Jonasch, E., Aldape, K., Liu, J., James, R. D., Ferguson, C. G., Xu, Y., Prestwich, G. D., and Mills, G. B. (2004) Lysophosphatidic acid production and action: validated targets in cancer? *J. Cell Biochem. 92*, 1115-1140.

(3) Carley, A. N., and Severson, D. L. (2005) Fatty acid metabolism is enhanced in type 2 diabetic hearts. *Biochim. Biophys. Acta 1734*, 112-126.

(4) Brandenburg, K., and Wiese, A. (2004) Endotoxins: relationships between structure, function, and activity. *Curr. Top. Med. Chem. 4*, 1127-1146.

(5) Michikawa, M. (2004) Neurodegenerative disorders and cholesterol. *Curr. Alzheimer Res. 1*, 271-275.

(6) Brown, A. J., and Jessup, W. (1999) Oxysterols and atherosclerosis. *Atherosclerosis 142*, 1-28.

(7) Radeff-Huang, J., Seasholtz, T. M., Matteo, R. G., and Brown, J. H. (2004) G protein mediated signaling pathways in lysophospholipid induced cell proliferation and survival. *J. Cell Biochem. 92*, 949-966.

(8) Abdel Ghani, E. M., Weis, S., Walev, I., Kehoe, M., Bhakdi, S., and Palmer, M. (1999) Streptolysin O: inhibition of the conformational change during membrane binding of the monomer prevents oligomerization and pore formation. *Biochemistry 38*, 15204-15211.

(9) Cho, W., and Stahelin, R. V. (2005) Membrane-protein interactions in cell signaling and membrane trafficking. *Annu. Rev. Biophys. Biomol. Struct. 34*, 119-151.

(10) Kazlauskaite, J., and Pinheiro, T. J. (2005) Aggregation and fibrillization of prions in lipid membranes. *Biochem. Soc. Symp. 72*, 211-222.

(11) Mukherjee, S., and Maxfield, F. R. (2004) Membrane domains. *Annu. Rev. Cell Dev. Biol. 20*, 839-866.

(12) Jelinek, R., and Kolusheva, S. (2005) Membrane interactions of host-defense peptides studied in model systems. *Curr. Protein Pept. Sci. 6*, 103-114.

(13) Brezesinski, G., and Mohwald, H. (2003) Langmuir monolayers to study interactions at model membrane surfaces. *Adv. Colloid Interface Sci. 100-102*, 563-584.

(14) Chattopadhyay, A. (2003) Exploring membrane organization and dynamics by the wavelength-selective fluorescence approach. *Chem. Phys. Lipids 122*, 3-17.

(15) Mintzer, E. A., Waarts, B., Wilschut, J., and Bittman, R. (2001) Behavior of a photoactivatable analog of cholesterol, 6-photocholesterol, in model membranes. *FEBS Lett. 510*, 181-184.

(16) Siems, W., Quast, S., Carluccio, F., Wiswedel, I., Hirsch, D., Augustin, W., Hampi, H., Riehle, M., and Sommerburg, O. (2002) Oxidative stress in chronic renal failure as a cardiovascular risk factor. *Clin. Nephol. 58*, S12-S19.

(17) Salvayre, R., Auge, N., Benoist, H., and Negre-Salvayre, A. (2002) Oxidized low-density lipoprotein-induced apoptosis. *Biochim. Biophys. Acta 1585*, 213-221.

(18) Li, Z., Mintzer, E. A., and Bittman, R. (2004) The critical micelle concentrations of lysophosphatidic acid and sphingosylphosphorylcholine. *Chem. Phys. Lipids 130*, 197-201.

(19) Bittman, R. (1997) Has nature designed the cholesterol side chain for optimal interaction with phospholipids?, in *Subcellular Biochemistry* (Bittman, R., Ed.) pp 145-171, Plenum, New York.

(20) Slotte, J. P. (1997) Cholesterol-sphingomyelin interactions in cells--effects on lipid metabolism, in *Subcellular Biochemistry* (Bittman, R., Ed.) pp 277-293, Plenum, New York.

(21) Ohvo-Rekila, H., Ramstedt, B., Leppima, P., and Slotte, J. P. (2002) Cholesterol interactions with phospholipids in membranes. *Prog. Lipid Res. 41*, 66-97.

(22) Palmer, M. (2004) Cholesterol and the activity of bacterial toxins. *FEMS Microbiol. Lett. 238*, 281-289.

(23) White, J., and Helenius, A. (1980) pH-dependent fusion between the Semliki Forest virus membrane and liposomes. *Proc. Natl. Acad. Sci. USA 77*, 3273-3277.

(24) Kielien, M. C., and Helenius, A. (1984) Role of cholesterol in fusion of Semliki Forest virus with membranes. *J. Virol. 52*, 281-283.

(25) Phalen, T., and Kielien, M. C. (1991) Cholesterol is required for infection by Semliki Forest virus. *J. Cell Biol. 112*, 615-623.

(26) Wahlberg, J. M., Bron, R., Wilschut, J., and Garoj, H. (1992) Membrane fusion of Semliki Forest virus involves homotrimers of the fusion protein. *J. Virol. 66*, 7309-7318.

(27) Bron, R., Wahlberg, J. M., Garoj, H., and Wilschut, J. (1993) Membrane fusion of Semliki Forest virus in a model system: correlation between fusion kinetics and structural changes in the envelope glycoprotein. *EMBO J. 12*, 693-701.

(28) Nieva, J. L., Bron, R., Corver, J., and Wilschut, J. (1994) Membrane fusion of Semliki Forest virus requires sphingolipids in the target membrane. *EMBO J. 13*, 2797-2804.

(29) Simons, K., and Ikonen, E. (1997) Functional rafts in cell membranes. *Nature 387*, 569-572.

(30) Simons, K., and Ikonen, E. (2000) How cells handle cholesterol. *Science 290*, 1721-1726.

(31) Butler, K. W., Smith, I. C. P., and Schneider, H. (1970) Sterol structure and ordering effects in spin-labelled phospholipid multibilayer structures. *Biochim. Biophys. Acta 219*, 514-517.

(32) Bayley, H. (1983) *Photogenerated Reagents in Biochemistry and Molecular Biology*, Elsevier, Amsterdam.

(33) Brunner, J. (1989) Photochemical labeling of apolar phase of membranes. *Methods Enzymol. 172*, 628-687.

(34) Matyash, V., Geier, C., Henske, A., Mukherjee, S., Hirsh, D., Thiele, C., Grant, B., Maxfield, F. R., and Kurzchalia, T. V. (2001) Distribution and transport of cholesterol in *Caenorhabditis elegans*. *Mol. Biol. Cell 12*, 1725-1736.

(35) Simons, M., Kramer, E. M., Thiele, C., Stoffel, W., and Trotter, J. (2000) Assembly of myelin by association of proteolipid protein with cholesterol- and galactosylceramide-rich membrane domains. *J. Cell Biol. 151*, 143-154.

(36) Eroglu, C., Brügger, B., Wieland, F., and Sinning, I. (2003) Glutamate-binding affinity of Drosophila metabotropic glutamate receptor is modulated by association with lipid rafts. *Proc. Natl. Acad. Sci. USA 100*, 10219-10224.

(37) Alpy, F., Latchumanan, V. K., Kedinger, V. K., Janoshazi, A., Thiele, C., Wendling, C., Rio, M. C., and Tomasetto, C. (2005) Functional characterization of the MENTAL domain. *J. Biol. Chem. 280*, 17945-17952.

(38) Chapman, D., Owens, N. F., Phillips, M. C., and Walker, D. A. (1969) Mixed monolayers of phospholipids and cholesterol. *Biochim. Biophys. Acta 183*, 458-465.

(39) Ghosh, D., Lyman, R. L., and Tinoco, J. (1971) Behavior of specific natural lecithins and cholesterol at the air water-interface. *Chem. Phys. Lipids 7*, 173-184.

(40) Cadenhead, D. A., and Müller-Landau, F. (1980) Molecular accommodation and molecular interactions in mixed insoluble monomolecular films. *J. Colloid Interface Sci. 78*, 269-270.

(41) Smit, J. M., Bittman, R., and Wilschut, J. (1999) Low-pH-dependent fusion of Sindbis virus with receptor-free cholesterol- and sphingolipid-containing liposomes. *J. Virol. 73*, 8476-8484.

(42) Thiele, C., Hannah, M. J., Fahrenholz, F., and Huttner, W. B. (2000) Cholesterol binds to synaptophysin and is required for biogenesis of synaptic vesicles. *Nat. Cell Biol. 2*, 42-49.

(43) Cruz, J. C., Thomas, M., Wong, E., Ohgami, N., Sugii, S., Curphey, T., Chang, C. C., and Chang, T. Y. (2002) Synthesis and biochemical properties of a new photoactivatable cholesterol analog 7,7-azocholestanol and its linoleate ester in Chinese hamster ovary cell lines. *J. Lipid Res. 43*, 1341-1347.

(44) Ohgami, N., Ko, D. C., Thomas, M., Scott, M. P., Chang, C. C., and Chang, T. Y. (2004) Binding between the Niemann-Pick C1 protein and a photoactivatable cholesterol analog requires a functional sterol-sensing domain. *Proc. Natl. Acad. Sci. USA 101*, 12473-12478.

(45) Phillips, M. C., Ladbrooke, B. D., and Chapman, D. (1970) Molecular interactions in mixed lecithin systems. *Biochim. Biophys. Acta 196*, 35-44.

(46) Phillips, M. C. (1972) The physical state of phospholipids and cholesterol in monolayers, bilayers and membranes. *Prog. Surface Membr. Sci. 4*, 139-221.

(47) Morrow, M. R., Singh, D., Lu, D., and Grant, C. W. M. (1995) Glycosphingolipid fatty acid arrangement in phospholipid bilayers: cholesterol effects. *Biophys. J. 68*, 179-186.

(48) De Kruijff, B., De Greef, W. J., Van Eyk, R. V. W., Demel, R. A., and Van Deenen, L. L. M. (1973) The effect of different fatty acid and sterol composition on the erythritol flux through the cell membrane of *Acholeplasma laidlawii*. *Biochim. Biophys. Acta 298*, 479-499.

(49) Lund-Katz, S., Laboda, H. M., McLean, L. R., and Phillips, M. C. (1988) Influence of molecular packing and phospholipid type on rates of cholesterol exchange. *Biochemistry 27*, 3416-3423.

(50) Slotte, J. P., Ostman, A. L., Kumar, E. R., and Bittman, R. (1993) Cholesterol interacts with lactosyl and maltosyl cerebrosides but not with glucosyl or galactosyl cerebrosides in mixed monolayers. *Biochemistry 32*, 7886-7892.

(51) Radhakrishnan, A., and McConnell, H. M. (2002) Thermal dissociation of condensed complexes of cholesterol and phospholipid *J. Phys. Chem. 106*, 4755-4762.

(52) Wiegand, V., Chang, T. Y., Strauss, J. F., Fahrenholz, F., and Gimpl, G. (2003) Transport of plasma membrane-derived cholesterol and the function of Niemann-Pick C1 Protein. *FASEB J. 17*, 782-784.

(53) Harikumar, K. G., and Miller, L. J. (2005) Fluorescence resonance energy transfer analysis of the antagonist- and partial agonist-occupied states of the cholecystokinin receptor. *J. Biol. Chem. 280*, 18631-18635.

(54) Lehto, M. T., and Sharom, F. J. (2002) Proximity of the protein moiety of a GPI-anchored protein to the membrane surface: a FRET study. *Biochemistry 41*, 8368-8376.

(55) Haustein, E., and Schwille, P. (2004) Single-molecule spectroscopic methods. *Curr. Opin. Struct. Biol. 14*, 531-540.

(56) Karolin, J., Johansson, L. B. A., Strandberg, L., and Ny, T. (1994) Fluorescence and absorption spectroscopic properties of dipyrronomethene boron difluoride (BODIPY) derivatives in liquids, lipid membranes, and proteins. *J. Am. Chem. Soc. 116*, 7801-7806.

(57) Kurata, S., Kanagawa, T., Yamada, Y., Torimura, M., Yokomaku, T., Kamagata, Y., and Kurane, R. (2001) Fluorescent quenching-based quantitative detection of specific DNA/RNA using a BODIPY((R)) FL-labeled probe or primer. *Nucleic Acids Res. 29*, e34.

(58) Bergström, F., Hagglof, P., Karolin, J., Ny, T., and Johansson, L. B. (1999) The use of site-directed fluorophore labeling and donor-donor energy migration to investigate solution structure and dynamics in proteins. *Proc. Natl. Acad. Sci. USA 96*, 12477-12481.

(59) DiCesare, N., and Lakowicz, J. R. (2001) Spectral properties of fluorophores combining the boronic acid group with electron donor or withdrawing groups. Implication in the development of fluorescence probes for saccharides. *J. Phys. Chem. 105*, 6834-6840.

(60) Ohvo-Rekila, H., and Slotte, J. P. (1996) Cyclodextrin-mediated removal of sterols from monolayers: effects of sterol structure and phospholipids on desorption rate. *Biochemistry 35*, 8018-8024.

(61) Li, X., Momsen, M. M., Smaby, J. M., Brockman, H. L., and Brown, R. E. (2001) Cholesterol decreases the interfacial elasticity and detergent solubility of sphingomyelins. *Biochemistry 40*, 5954-5963.

(62) Xu, X., and London, E. (2000) The effect of sterol structure on membrane lipid domains reveals how cholesterol can induce lipid domain formation. *Biochemistry 39*, 843-849.

(63) Kauffman, J. M., Westerman, P. W., and Carey, M. C. (2000) Fluorocholesterols, in contrast to hydroxycholesterols, exhibit interfacial properties similar to cholesterol. *J. Lipid Res. 41*, 991-1003.

(64) Theunissen, J. J., Jackson, R. L., Kempen, H. J., and Demel, R. A. (1986) Membrane properties of oxysterols. Interfacial orientation, influence on membrane permeability and redistribution between membranes. *Biochim. Biophys. Acta 860*, 66-74.

(65) Mendelsohn, R., Davies, M. A., Schuster, H. F., Xu, Z. C., and Bittman, R. (1991) CD2 rocking modes as quantitative infrared probes of one-, two-, and three-bond conformational disorder in dipalmitoylphosphatidylcholine and dipalmitoylphosphatidylcholine/cholesterol mixtures. *Biochemistry 30*, 8558-8563.

(66) Ahmed, S. N., Brown, D. A., and London, E. (1997) On the origin of sphingolipid/cholesterol-rich detergent-insoluble cell membranes: physiological concentrations of cholesterol and sphingolipid induce formation of a detergent-insoluble, liquid-ordered lipid phase in model membranes. *Biochemistry 36*, 10944-10953.

(67) Wang, J., Megha, and London, E. (2004) Relationship between sterol/steroid structure and participation in ordered lipid domains (lipid rafts): implications for lipid raft structure and function. *Biochemistry 43*, 1010-1018.

(68) Watson, P., Jones, A. T., and Stephens, D. J. (2005) Intracellular trafficking pathways and drug delivery: fluorescence imaging of living and fixed cells. *Adv. Drug Deliv. Rev. 57*, 43-61.

(69) Pownell, H. J., and Smith, L. C. (1989) Pyrene-labeled lipids: versatile probes of membrane dynamics in vitro and in living cells. *Chem. Phys. Lipids 50*, 191-211.

(70) Lentz, B. R. (1993) Use of fluorescent probes to monitor molecular order and motions within liposome bilayers. *Chem. Phys. Lipids 64*, 99-116.

(71) Mukherjee, S., and Chattopadhyay, A. (2005) Monitoring cholesterol organization in membranes at low concentrations utilizing the wavelength-selective fluorescence approach. *Chem. Phys. Lipids 134*, 79-84.

(72) Scheidt, H. A., Muller, P., Herrmann, A., and Huster, D. (2003) The potential of fluorescent and spin-labeled steroid analogs to mimic natural cholesterol. *J. Biol. Chem. 278*, 45563-45569.

(73) Loura, L. M. S., Fedorov, A., and Prieto, M. (2001) Exclusion of a cholesterol analog from the cholesterol-rich phase in model membranes. *Biochim. Biophys. Acta 1511*, 236-243.

(74) Asuncion-Punzalan, E., Kachel, K., and London, E. (1998) Groups with polar characteristics can locate at both shallow and deep locations in membranes: the behavior of dansyl and related probes. *Biochemistry 37*, 4603-4611.

(75) Wenz, J. J., and Barrantes, F. J. (2003) Steroid structural requirements for stabilizing or disrupting lipid domains. *Biochemistry 42*, 14267-14276.

(76) Crowder, C. M., Westover, E. J., Kumar, A. S., Ostlund, R. E., and Covey, D. F. (2001) Enantiospecificity of cholesterol function in vivo. *J. Biol. Chem. 276*, 44369-44372.

(77) Arnett, E., Gold, J., Harvey, N., Johnson, E., and Whitesell, L. (1988) Stereoselective recognition in phospholipid monolayers. *Adv. Exp. Med. Biol. 238*, 21-26.

(78) Geva, M., Izhaky, D., Mickus, D. E., Rychnovsky, S. D., and Addadi, L. (2001) Stereoselective recognition of monolayers of cholesterol, ent-cholesterol, and epicholesterol by an antibody. *ChemBioChem. 2*, 265-271.

(79) Rychnovsky, S. D., and Mickus, D. E. (1992) Synthesis of *ent*-cholesterol, the unnatural enantiomer. *J. Org. Chem. 57*, 2732-2736.

(80) Jiang, X., and Covey, D. F. (2002) Total synthesis of ent-cholesterol via a steroid C,D-ring side-chain synthon. *J. Org. Chem. 67*, 4893-4900.

(81) Epand, R. M., Rychnovsky, S. D., Belani, J. D., and Epand, R. F. (2005) Role of chirality in peptide-induced formation of cholesterol-rich domains. *Biochem. J. 390*, 541-548.

(82) Westover, E. J., Covey, D. F., Brockman, H. L., Brown, R. E., and Pike, L. J. (2003) Cholesterol depletion results in site-specific increases in epidermal growth factor receptor phosphorylation due to membrane level effects. Studies with cholesterol enantiomers. *J. Biol. Chem. 278*, 51125-51133.

(83) Mannock, D. A., McIntosh, T. J., Jiang, X., Covey, D. F., and McElhaney, R. N. (2003) Effects of natural and enantiomeric cholesterol on the thermotropic phase behavior and structure of egg sphingomyelin bilayer membranes. *Biophys. J. 84*, 1038-1046.

(84) Lalitha, S., Kumar, A. S., Stine, K. J., and Covey, D. F. (2001) Chirality in membranes: First evidence that enantioselective interactions between cholesterol and cell membrane lipids can be a determinant of membrane physical properties. *Supramol. Chem. 1*, 53-61.

(85) Zitzer, A., Westover, E. J., Covey, D. F., and Palmer, M. (2003) Differential interaction of the two cholesterol-dependent, membrane-damaging toxins, Streptolysin O and *Vibrio cholerae* cytolysin, with enantiomeric cholesterol. *FEBS Lett. 553*, 229-231.

(86) van Meer, G., and Simons, K. (1988) Lipid polarity and sorting in epithelial cells. *J. Cell Biochem. 36*, 51-58.

(87) Anderson, R. G. (1998) The caveolae membrane system. *Annu. Rev. Biochem. 67*, 199-225.

(88) Sheets, E. D., Holowka, D., and Baird, B. (1999) Critical role for cholesterol in Lyn-mediated tyrosine phosphorylation of FcepsilonRI and their association with detergent-resistant membranes. *J. Cell Biol. 145*, 877-887.

(89) Stulnig, T. M., Berger, M., Sigmund, T., Raederstorff, D., Stockinger, H., and Waldhausl, W. (1998) Polyunsaturated fatty acids inhibit T cell signal transduction by modification of detergent-insoluble membrane domains. *J. Cell Biol. 143*, 637-644.

(90) Yamabhai, M., and Anderson, R. G. (2002) Second cysteine-rich region of epidermal growth factor receptor contains targeting information for caveolae/rafts. *J. Biol. Chem. 277*, 24842-24846.

(91) Hooper, N. M. (1999) Detergent-insoluble glycosphingolipid/cholesterol-rich membrane domains, lipid rafts and caveolae (review). *Mol. Membr. Biol. 16*, 145-156.

(92) Brown, D. A., and Rose, J. K. (1992) Sorting of GPI-anchored proteins to glycolipid-enriched membrane subdomains during transport to the apical cell surface. *Cell 68*, 533-544.

(93) Sankaram, M. B., and Thompson, T. E. (1990) Interaction of cholesterol with various glycerophospholipids and sphingomyelin. *Biochemistry 29*, 10670-10675.

(94) Almeida, P. F., Vaz, W. L., and Thompson, T. E. (1992) Lateral diffusion in the liquid phases of dimyristoylphosphatidylcholine/cholesterol lipid bilayers: a free volume analysis. *Biochemistry 31*, 6739-6747.

(95) Xu, X., Bittman, R., Duportail, G., Heissler, D., Vilcheze, C., and London, E. (2001) Effect of the structure of natural sterols and sphingolipids on the formation of ordered sphingolipid/sterol domains (rafts). Comparison of cholesterol to plant, fungal, and disease-associated sterols and comparison of sphingomyelin, cerebrosides, and ceramide. *Biochemistry 276*, 33540-33546.

(96) Gaus, K., Dean, R. T., Kritharides, L., and Jessup, W. (2001) Inhibition of cholesterol efflux by 7-ketocholesterol: comparison between cells, plasma membrane vesicles, and liposomes as cholesterol donors. *Biochemistry 40*, 13002-13014.

(97) Verhagen, J. C., ter Braake, P., Teunissen, J., van Ginkel, G., and Sevanian, A. (1996) Physical effects of biologically formed cholesterol oxidation products on lipid membranes investigated with fluorescence depolarization spectroscopy and electron spin resonance. *J. Lipid Res. 37*, 1488-1502.

(98) Berthier, A., Lemaire-Ewing, S., Prunet, C., Monier, S., Athias, A., Bessede, G., Pais de Barros, J. P., Laubriet, A., Gambert, P., Lizard, G., and Neel, D. (2004) Involvement of a calcium-dependent dephosphorylation of BAD associated with the localization of Trpc-1 within lipid rafts in 7-ketocholesterol-induced THP-1 cell apoptosis. *Cell Death Differ. 11*, 897-905.

(99) Kucuk, O., Lis, L. J., Dey, T., Mata, R., Westerman, M. P., Yachnin, S., Szostek, R., Tracy, D., Kauffman, J. W., and Gage, D. A. (1992) The effects of cholesterol oxidation products in sickle and normal red blood cell membranes. *Biochim. Biophys. Acta 1103*, 296-302.

(100) Taylor, C. B., Peng, S. K., Werthessen, N. T., Tham, P., and Lee, K. T. (1979) Spontaneously occurring angiotoxic derivatives of cholesterol. *Am. J. Clin. Nutr. 32*, 40-57.

(101) Bischoff, P. L., Holl, V., Coelho, D., Dufour, P., Weltin, D., and Luu, B. (2000) Apoptosis at the interface of immunosuppressive and anticancer activities: the examples of two classes of chemical inducers, oxysterols and alkylating agents. *Curr. Med. Chem. 7*, 693-713.

(102) Reiss, A. B., Siller, K. A., Rahman, M. M., Chan, E. S., Ghiso, J., and de Leon, M. J. (2004) Cholesterol in neurologic disorders of the elderly: stroke and Alzheimer's disease. *Neurobiol. Aging 25*, 977-989.

(103) Schroeder, R., London, E., and Brown, D. A. (1994) Interactions between saturated acyl chains confer detergent resistance on lipids and glycosylphosphatidylinositol (GPI)-anchored proteins: GPI-anchored proteins in liposomes and cells show similar behavior. *Proc. Natl. Acad. Sci. USA 91*, 12130-12134.

(104) Radhakrishnan, A., and McConnell, H. M. (2000) Chemical activity of cholesterol in membranes. *Biochemistry 39*, 8119-8124.

(105) Siess, W., Zangl, K. J., Essler, M., Bauer, M., Brandl, R., Corrinth, C., Bittman, R., Tigyi, G., and Aepfelbacher, M. (1999) Lysophosphatidic acid mediates the rapid activation of platelets and endothelial cells by mildly oxidized low density lipoprotein and accumulates in human atherosclerotic lesions. *Proc. Natl. Acad. Sci. USA 96*, 6931-6936.

(106) English, D., Garcia, J. G., and Brindley, D. N. (2001) Platelet-released phospholipids link haemostasis and angiogenesis. *Cardiovasc. Res. 49*, 588-599.

(107) Pagés, C., Simon, M. F., Valet, P., and Saulnier-Blache, J. S. (2001) Lysophosphatidic acid synthesis and release. *Prostaglandins Other Lipid Mediat. 64*, 1-10.

(108) Goetzl, E. J., and An, S. (1998) Diversity of cellular receptors and functions for the lysophospholipid growth factors lysophosphatidic acid and sphingosine 1-phosphate. *FASEB J. 12*, 1589-1598.

(109) Chun, J., Contos, J. J., and Munroe, D. (1999) A growing family of receptor genes for lysophosphatidic acid (LPA) and other lysophospholipids (LPs). *Cell Biochem. Biophys. 30*, 213-242.

(110) Yu, F. X., Sun, H. Q., Janmey, P. A., and Yin, H. L. (1992) Identification of a polyphosphoinositide-binding sequence in an actin monomer-binding domain of gelsolin. *J. Biol. Chem. 267*, 14616-14621.

(111) Yin, H. L., Albrecht, J. H., and Fattoum, A. (1981) Identification of gelsolin, a Ca2+-dependent regulatory protein of actin gel-sol transformation, and its intracellular distribution in a variety of cells and tissues. *J. Cell Biol. 91*, 901-906.

(112) Bucki, R., Georges, P. C., Espinassous, Q., Funaki, M., Pastore, J. J., Chaby, R., and Janmey, P. A. (2005) Inactivation of endotoxin by human plasma gelsolin. *Biochemistry 44*, 9590-9597.

(113) Raetz, C. R. (1986) Molecular genetics of membrane phospholipid synthesis. *Annu. Rev. Genet. 20*, 253-295.

(114) Raetz, C. R. H. (1990) Biochemistry of endotoxins. *Annu. Rev. Biochem. 59*, 129-170.

(115) Raetz, C. R. H. (1993) Bacterial endotoxins: extraordinary lipids that activate eucaryotic signal transduction. *J. Bacteriol. 175*, 5745-5753.

(116) Lerouge, I., and Vanderleyden, J. (2002) O-antigen structural variation: mechanisms and possible roles in animal/plant-microbe interactions. *FEMS Microbiol. Rev. 26*, 17-47.

(117) Goetzl, E. J., Lee, H., Azuma, T., Stossel, T. P., Turck, C. W., and Karliner, J. S. (2000) Gelsolin binding and cellular presentation of lysophosphatidic acid. *J. Biol. Chem. 275*, 14573-14578.

(118) Xian, W., and Janmey, P. A. (2002) Dissecting the gelsolin-polyphosphoinositide interaction and engineering of a polyphosphoinositide-sensitive gelsolin C-terminal half protein. *J. Mol. Biol. 322*, 755-771.

(119) Stossel, T. P. (1993) On the crawling of animal cells. *Science 260*, 1086-1094.

(120) Janmey, P. A. (1994) Phosphoinositides and calcium as regulators of cellular actin assembly and disassembly. *Annu. Rev. Physiol. 56*, 169-191.

(121) Janmey, P. A., Lamb, J., Allen, P. G., and Matsudaira, P. T. (1992) Phosphoinositide-binding peptides derived from the sequences of gelsolin and villin. *J. Biol. Chem. 267*, 11818-11823.

(122) Meerschaert, K., De Corte, V., De Ville, Y., Vandekerckhove, J., and Gettemans, J. (1998) Gelsolin and functionally similar actin-binding proteins are regulated by lysophosphatidic acid. *EMBO J. 17*, 5923-5932.

(123) David, S. A. (2001) Towards a rational development of anti-endotoxin agents: novel approaches to sequestration of bacterial endotoxins with small molecules. *J. Mol. Recognit. 14*, 370-387.

(124) Juan, T. S., Hailman, E., Kelley, M. J., Busse, L. A., Davy, E., Empig, C. J., Narhi, L. O., Wright, S. D., and Lichenstein, H. S. (1995) Identification of a lipopolysaccharide binding domain in CD14 between amino acids 57 and 64. *J. Biol. Chem. 270*, 5219-5224.

(125) Kirkland, T. N., Finley, F., Leturcq, D., Moriarty, A., Lee, J. D., Ulevitch, R. J., and Tobias, P. S. (1993) Analysis of lipopolysaccharide binding by CD14. *J. Biol. Chem. 268*, 24818-24823.

(126) Triantafilou, M., and Triantafilou, K. (2005) The dynamics of LPS recognition: complex orchestration of multiple receptors. *J. Endotoxin Res. 11*, 5-11.

(127) Brandenburg, K., David, A., Howe, J., Koch, M. H., Andra, J., and Garidel, P. (2005) Temperature dependence of the binding of endotoxins to the polycationic peptides polymyxin B and its nonapeptide. *Biophys. J. 88*, 1845-1858.

(128) Heerklotz, H., and Epand, R. M. (2001) The enthalpy of acyl chain packing and the apparent water-accessible apolar surface area of phospholipids. *Biophys. J. 80*, 271-279.

(129) Gallagher, K., and Sharp, K. (1998) Electrostatic contributions to heat capacity changes of DNA-ligand binding. *Biophys. J. 75*, 769-776.

(130) Garidel, P., and Blume, A. (1999) Interaction of alkaline earth cations with the negatively charged phospholipid 1,2-dimyristoyl-*sn*-glycero-3-phosphoglycerol: A differential scanning and isothermal titration calorimetric study *Langmuir 15*, 5526-5534.

(131) Corsico, B., Franchini, G. R., Hsu, K., and Storch, J. (2005) Fatty acid transfer from intestinal fatty acid binding protein to membranes: electrostatic and hydrophobic interactions. *J. Lipid Res. 46*, 1765-1772.

(132) Murakami, N., Yokomizo, T., Okuno, T., and Shimizu, T. (2004) G2A is a proton-sensing G-protein-coupled receptor antagonized by lysophosphatidylcholine. *J. Biol. Chem. 279*, 42484-42491.

(133) Dahl, B., Schiodt, F. V., Ott, P., Gvozdenovic, R., Yin, H. L., and Lee, W. M. (1999) Plasma gelsolin is reduced in trauma patients. *Shock 12*, 102-104.

(134) Tigyi, G., and Parrill, A. L. (2003) Molecular mechanisms of lysophosphatidic acid action. *Prog. Lipid Res. 42*, 498-526.

(135) Meyer zu Heringdorf, D., Himmel, H. M., and Jakobs, K. H. (2002) Sphingosylphosphorylcholine-biological functions and mechanisms of action. *Biochim. Biophys. Acta 1582*, 178-189.

(136) Bektas, M., Barak, L. S., Jolly, P. S., Liu, H., Lynch, K. R., Lacana, E., Suhr, K.-B., Milstien, S., and Spiegel, S. (2003) The G protein-coupled receptor GPR4 suppresses ERK activation in a ligand-independent manner. *Biochemistry 42*, 12181-12191.

(137) Heerklotz, H., and Seelig, J. (2000) Titration calorimetry of surfactant–membrane partitioning and membrane solubilization. *Biochim. Biophys. Acta 1508*, 69-85.

(138) Patist, A. (2002) Determining critical micelle concentration., in *Handbook of Applied Surface and Colloid Chemistry* (Holmberg, K., Ed.) pp 239-249, Wiley, Chichester, UK.

(139) Lasch, J., and Hildebrand, A. (2002) Isothermal titration calorimetry to study CMCs of neutral surfactants of the liposome-forming bolaamphiphile dequalinium. *J. Liposome Res. 12*, 51-56.

(140) Moolenaar, W. H. (1999) Bioactive lysophospholipids and their G protein-coupled receptors. *Exp. Cell Res. 253*, 230-238.

(141) Moolenaar, W. H. (2000) Development of our current understanding of bioactive lysophospholipids. *Ann. N.Y. Acad. Sci. 905*, 1-10.